Distribution Agreement

In presenting this thesis as a partial fulfillment of the requirements for a degree from Emory University, I hereby grant to Emory University and its agents the non-exclusive license to archive, make accessible, and display my thesis in whole or in part in all forms of media, now or hereafter now, including display on the World Wide Web. I understand that I may select some access restrictions as part of the online submission of this thesis. I retain all ownership rights to the copyright of the thesis. I also retain the right to use in future works (such as articles or books) all or part of this thesis.

Jacqueline Steele April 4, 2018

Developmental Changes in the Visual Processing of Trustworthy and Untrustworthy Faces

by

Jacqueline Steele

Mar Sanchez PhD.
Adviser

Neuroscience and Behavioral Biology

Mar Sanchez PhD.

Adviser

Jocelyne Bachevalier PhD.

Committee Member

Sarah Shultz PhD.

Committee Member

2018

Developmental Changes in the Visual Processing of Trustworthy and Untrustworthy Faces

By

Jacqueline Steele

Mar Sanchez PhD.

Adviser

An abstract of
a thesis submitted to the Faculty of Emory College of Arts and Sciences
of Emory University in partial fulfillment
of the requirements of the degree of
Bachelor of Sciences with Honors

Neuroscience and Behavioral Biology

2018

Abstract

Developmental Changes in the Visual Processing of Trustworthy and Untrustworthy Faces
By Jacqueline Steele

Reading others' facial cues (i.e. trustworthiness) in social interactions is crucial to understanding their intentions and emotions, and is impaired in individuals with Autism Spectrum Disorder (ASD). Characterizing the emergence and development of this skill and supporting brain regions may further broaden our understanding of impaired socioemotional development observed in children with ASD. Rhesus macaques, a highly translational nonhuman primate model of early socioemotional development, allow for densely sampled longitudinal neuroimaging studies not feasible in human infants. Therefore, this study aims to characterize early development of social and facial feature perception and the underlying brain regions in rhesus infants. We conducted analyses of eye-tracking and MRI data collected longitudinally in 31 infant male macaques (1week – 24 weeks) living with their mothers in complex social groups. Each eye-tracking session included trials of 2 human and 2 monkey faces representing extreme levels of trustworthiness. Looking behavior, including fixation to eye and mouth regions was characterized for trustworthy and untrustworthy faces. Structural MRI scans sequences acquired using a 3T scanner were used to characterize volumetric changes of the prefrontal cortex (PFC), the temporo-parieto-occipital junction (TPO) of the superior temporal sulcus (STS), inferotemporal area (TE), insula, and amygdala (AMY)- all areas involved in visual processing of "trust" in faces. Our sMRI results show region specific developmental growth trajectories. Our eye-tracking results show that when viewing faces, the subjects preferentially looked at untrustworthy eyes in comparison to trustworthy eyes regardless of the stimuli species. Also, the subjects show a significant decline in the amount of time spent looking at human faces at 9 weeks of age in comparison to 5 and 21 weeks of age. This age range corresponds to an age

range (8-16 weeks of age) where the AMY, TE, PFC, and insula show slowing in their growth. Our results parallel the developmental trajectories of social visual engagement in human infants (Jones & Klin, 2013), and further validate rhesus monkeys as a translational model of early socioemotional development.

Developmental Changes in the Visual Processing of Trustworthy and Untrustworthy Faces

By

Jacqueline Steele

Mar Sanchez PhD.

Adviser

A thesis submitted to the Faculty of Emory College of Arts and Sciences
of Emory University in partial fulfillment
of the requirements of the degree of
Bachelor of Sciences with Honors

Neuroscience and Behavioral Biology

2018

Acknowledgements

I would like to thank Dr. Mar Sanchez for being a terrific mentor and teacher throughout this process. The many hours you spent in meetings with me and the feedback you provided on my writing and presentations was invaluable. The opportunity to contribute to meaningful research in conjunction with your guidance has not only taught me about how to work in a lab, but enabled me to pursue my career goals. Thank you for pushing me to investigate findings at a deeper level and challenge myself into writing the best thesis I could produce. I admire your hard work and dedication to science, and I will strive to emulate those qualities in my own career.

I would also like to thank post-doctoral fellow Zsofia Kovacs-Balint for her mentorship throughout this project, and over the last 3 ½ years. You have helped me learn many lab techniques like how to manually edit masks, run AutoSeg, and conduct statistical analysis. Thank you for teaching me many important skills and helping me grow as a research student. You were always available to answer any questions anytime of the day or night. Thank you for being a great colleague, teacher and friend.

I would also like to thank Zeena Ammar and Christa Payne for their help with processing the eye-tracking data. In addition, I would like to thank Dr. Jocelyne Bachevalier and Dr. Sarah Shultz for their serving on my committee and taking time to provide their feedback on this thesis. Lastly, I would like to thank the NBB department and Dr. Leah Roesch for their support as I took on this project.

Table of Contents

Table of Figures

Introduction:

Humans use faces to identify people, as well as to detect their emotions, attention, intentions, and trustworthiness. Judgments of these characteristics influence people's behavior during social interactions (Frith 2009). The way in which typically developing individuals and individuals with autism spectrum disorder (ASD) process faces and use this information to modify their behavior in social interactions is different, with the hallmark of ASD being impairment in social functioning (Wing and Gould 1979). People with ASD avoid eye contact and have a general preference for inanimate objects over faces, whereas typically developing individuals prefer looking at faces over objects (Schultz et al. 2000). Adults with ASD have also been found to process faces in individual sections, whereas healthy adults process faces holistically; for example, previous research has shown that individuals with ASD are less sensitive to the face inversion effect or the misalignment of face parts than their healthy counterparts (Dakin and Frith 2005; Gauthier et al. 2009; Joseph and Tanaka 2003; Yi et al. 2013b). Notably, individuals with ASD have difficulty reading facial expressions, which can cause them to miss social cues (Schultz et al. 2000) and make false judgements about trustworthiness.

These behavioral differences between typically developing individuals and individuals with ASD are already present in childhood. Typically developing children's judgements of trustworthiness change significantly during their preschool years (Ma et al. 2016), with the ability to start assessing trustworthiness based on facial cues emerging around age 5 – elementary school age (Ewing et al. 2015b). At that age, young children also use similar strategies to adults in judging facial features indicating trustworthiness (Ma et al. 2016) and are able to categorize faces as "nice," "strong," and "mean" with the same accuracy as adults

(Cogsdill et al. 2014). In contrast, preschool aged children's judgements of trustworthiness are based more on attractiveness than those of adults. (Ma et al. 2016). Judgements of adults with ASD are also more affected by the attractiveness of faces and their facial expressions when determining trustworthiness than typically developing adults, resembling patterns more similar to that of very young, typically developing children (Ma et al. 2016). From a behavioral perspective, children with ASD are less likely to distrust others after being repeatedly deceived than their typically developing counterparts (Yi et al. 2013a). Children with ASD also have difficulties integrating facial trustworthiness cues into their social interactions. For example, one study showed that while playing an economic game, children with ASD are equally likely to place their trust in people with trustworthy faces as they are in people with untrustworthy faces; whereas typically developing children are more likely to place their trust in people with trustworthy faces (Ewing et al. 2015b).

It would be important to conduct a longitudinal neuroimaging study to identify the neurodevelopmental changes associated with the switch in the way children assess trustworthiness from faces when they transition to school age (approx. 5 years) and with the differences between typically developing children and those with ASD. However, this type of study would be difficult in human infants due to ethical, safety, and procedural constraints (Bauman et al. 2013). As an interesting alternative, translational nonhuman primate (NHP) animal models can be used to understand the neurobiological changes underlying these transitions in early socioemotional development.

Non-Human Primate Model

The ability to identify and process faces and facial expressions and to judge intention or trustworthiness is also critical to NHP species, such as the rhesus macaque, due to their complex

social system with strict social hierarchy. During situations involving mate competition, for example, dominant male macaques are hypervigilant and jealous when they watch a subordinate mating with an estrous female, which would be considered a breach of trust by the subordinate (Rilling et al. 2004). Deceit is also observed as part of food competition. Subordinate macaques also show deceitful behaviors by collecting food quietly, to avoid drawing the attention from potential competitors, including humans (Santos et al. 2006).

Macaques social decisions, as in humans, are heavily reliant on information from faces and other body features. Previous research has demonstrated that male macaques forfeit a reward in exchange for the opportunity to view the faces of high-status monkeys from their social group, but require an extra-reward to view the faces of low-status monkeys (Deaner et al. 2005). This suggests that macaques may prefer to look at the faces of dominant animals because they have a higher valence (i.e. they need to pay attention to the faces in order to avoid aggression). They may also do this to determine opportunities to change their behavior in response to power dynamics. Face judgments are also used by macaques to determine social tolerance during play (Dobson 2012). A previous study showed that more tolerant macaques use a wider variety of facial expressions during play than less tolerant macaques; the more tolerant macaques exhibit a wider variety of facial expressions to signals to the playmate that they are open to interaction and negotiation (Dobson 2012). This suggests that the monkeys would be monitoring the faces of their playmates to determine whether or not to interact with them. Expanding on the idea of viewing faces to determine tolerant behavior, another study showed macaque and human subjects videos of cooperative and aggressive social interactions of humans, macaques, and other primates. When compared to each other, the macaque subjects' gaze behavior was qualitatively similar to that of humans, especially when viewing aggressive interactions. Both humans and

macaques looked predominantly at the faces of the aggressors in the videos when inspecting the individuals involved in the interaction, regardless of the species involved in the conflict (McFarland et al. 2013). Furthermore, when viewing stimuli in a simple social context, such as still images of faces, previous studies have shown that the gaze behavior of monkeys is similar to that of humans during free-viewing. For example, both species fixate the longest on the socially informative facial features, such as the eyes, nose and mouth (Dahl et al. 2009; Guo et al. 2003; Guo et al. 2010), and demonstrate a face-specific natural gaze bias to the left hemi-face (Guo et al. 2009). Finally, faces become important social stimuli at an early age in macaques. Infant macaques who receive more face-to-face contact during infancy display increased social interest at 2 months of age (Dettmer et al. 2016b). Taken together, previous research suggests that macaques use faces as important cues during social interactions to determine the intention and whether or not "to trust" (trustworthiness) other members of the group during these interactions. These behavioral similarities, along with anatomical similarities in brain structure, function, and development, make *Rhesus macaques* an ideal NHP species for these studies.

Brain Regions of Interest

Similar brain regions are thought to be involved in the ability to detect trustworthiness in humans and macaques. Past research has identified specific areas of the brain involved in face processing, and has demonstrated that these face specific networks are embedded in larger social networks that make decisions about behavior (Schwiedrzik et al. 2015). These social networks include regions such as the superior temporal sulcus (STS), prefrontal cortex (PFC), inferotemporal area (TE), the amygdala (AMY), and insula, all of which play important roles in determining the trustworthiness of individuals based on their faces and will be used as the regions of interests (ROIs) in this study. It has been reported that the STS and PFC are activated

during joint attention tasks in healthy adults, and less activated during these tasks in adults with ASD (Redcay et al. 2013). However, PFC activation is not used in joint attention during childhood and adolescence of typically developing children (Oberwelland et al. 2017), suggesting that a different neural network supports this skill during development than in adults. Previous research has also shown that the PFC is involved in the evaluation of trustworthiness by making judgement based largely on behavioral cues, rather than just faces themselves (Baron et al. 2011); therefore, building up a repertoire of behaviors that are considered trustworthy versus untrustworthy would take years of trial and error in social interactions. This PFC function, in conjunction with the PFC's protracted development (coming "online" later) suggests that it follows a different developmental trajectory than the STS in relation to judging trustworthiness, requiring years of social experience to affect the way the PFC processes social information. Additional evidence that the STS is involved in making judgements about trustworthiness comes from human studies of male faces, where that ability is interrupted when transcranial magnetic stimulation (TMS) is applied to the STS (Dzhelyova et al. 2011). Also, a functional magnetic resonance imaging (fMRI) study showed that the right STS was preferentially activated when judging the trustworthiness of faces, rather than other features, such as judging if the face belonged to a high school or college student. In this study, the posterior portion of the STS was particularly activated (Winston et al. 2002). A different fMRI study found similar results, when healthy human adults were asked to make judgments of trustworthy and untrustworthy faces, a circuit of the fusiform gyrus, STS, AMY, and insula were activated (Pinkham et al. 2008).

Interestingly, another human fMRI study revealed that the AMY and the insula are more active when judging a face as untrustworthy, in comparison to when faces were judged as trustworthy (Santos et al. 2016; Winston et al. 2002), potentially evaluating risk or threat in the

social interaction. Of potential relevance for the developmental emergence of trustworthiness judgement in children over 5 years of age, the AMY functional connectivity (FC) with other cortical areas in these social networks changes significantly from age 4 to adolescence. Specifically, the FC between the amygdala and medial PFC increases, while the FC between the amygdala and the STS and insula decreases with age (Gabard-Durnam et al. 2014). Finally, in a study of patients with AMY lesions, the subjects rated unfamiliar individuals more trustworthy and approachable than control subjects, and were less likely to judge a face to be unapproachable and untrustworthy (Adolphs et al. 1998), supporting the important role of the AMY in assessment of trustworthiness in social interactions.

Apart from the evolutionary advantages of detecting trustworthiness in faces during social interactions to evaluate the risk or threat to trust a conspecific, other functions are clearly involved, such as deciding who to cooperate with in order to increase personal benefits or reward. In this sense, studies in NHPs, including macaques, have highlighted the critical role that the PFC plays in expected reward, and response inhibition (Leon and Shadlen 1999; Sakagami et al. 2001). The ability to judge expected rewards is, indeed, connected to judging trustworthiness. For example, in order to determine whether to cooperate with someone to receive the maximum reward, and individual first needs to determine trustworthiness. Evaluating expected rewards as a result of cooperation is a function of the monkey PFC similar to that reported in the human PFC (Rae et al. 2015; Rowe et al. 2008), supporting the potential of the PFC's role in macaques ability to judge trustworthiness, similarly to the human PFC's involvement in this function (Prevost et al. 2015).

The STS, AMY, and insula of macaques may also play a similar role in judging trustworthiness as these ROIs in humans. The STS, amygdala, and insula are activated in

dominant male macaques while they are monitoring the behavior of subordinate's animals mating with an estrous female (Rilling et al. 2004). In this study, both the anterior and posterior portions of the STS were activated. Rilling and collaborators suggest that this increased activation is caused by the hypervigilance and "jealousy" of the dominant male macaque to the social interaction between the subordinate male and estrous female (Rilling et al. 2004). In general, the STS is thought to be involved in detecting the intentions of others (Frith and Frith 1999) and neurophysiological recordings in NHPs show that the STS is an association cortex critical for processing of socially relevant information with emotional valence and in monitoring conspecifics' behavior (Brothers 1990). As trustworthiness is a type of socially relevant information with emotional valence, the macaque STS could be involved in the ability to determine trustworthiness.

In humans, the fusiform gyrus plays an important role in face recognition and reading facial expressions. Previous studies show that the fusiform gyrus responds differentially to facial expressions, with distinct evoked potentials occurring for distinct expressions (Harry et al. 2013). Also, as mentioned above, this area is also involved in determining the trustworthiness of faces. In monkeys, the anatomical correlate of the fusiform gyrus is considered to be TE (Schwiedrzik et al. 2015). Similarly to the fusiform gyrus, this area is preferentially activated when viewing faces, over places and objects (Ungerleider et al. 1998). It has also been shown that area TE has similar face patch regions to the fusiform gyrus (Tsao et al. 2008).

The AMY is another important region in this social network, involved in threat detection of social stimuli as well as in the emotional/fear/anxiety responses to social stimuli (Bachevalier et al. 2016). It was also involved in the "jealousy" responses described above in dominant male macaques while watching a subordinate male mate with a receptive female (Rilling et al. 2004).

Threat detection and jealousy responses are related to determining trustworthiness in that untrustworthy faces would be considered threatening and untrustworthy actions could cause jealously.

The insula, another important brain region in social networks, is involved in the perception of visceral responses to socioemotional stimuli and keeps track of visceral responses in the body to stimuli (Stephani et al. 2011). Furthermore, in macaques, stimulation of the insula has been found to elicit different emotional facial expressions, such as lip smacking and disgust-related behaviors (Jezzini et al. 2015); it is suggested that this implies that the insula plays a role in automatic social behaviors in addition to somatosensory responses (Jezzini et al. 2015). Previous work also shows that the insula plays a role in reward expectations (like the PFC) (Mizuhiki et al. 2012), which can be related to being able to judge trustworthiness. Given the inusla's function in both visceral and social responses, it is possible that the insula contributes to responding to untrustworthy faces in macaques as it does in humans (Santos et al. 2016; Winston et al. 2002).

Now, what makes a face trustworthy or not? When examining trustworthy faces as a stimulus, facial features that are evaluated as trustworthy are often considered feminine, or baby-like (Wincenciak et al. 2015). From an evolutionary perspective this is important because humans need to trust their mothers and offspring in order to survive. The trustworthy facial characteristics are considered to be more sincere and even neutral trustworthy faces show an undertone of happiness; whereas untrustworthy facial features tend to look more tense and show undertones of anger or sadness (Engell et al. 2010). With this being said, trustworthy scores are not solely based on emotional expressions. In a critical study that demonstrated this point, an experiment showed trustworthy and untrustworthy faces to the participants that also had overt

emotional facial expressions. The results showed that faces with expressions of 'disgust,' 'fear,' and 'surprise' received the same trustworthy score as faces with 'neutral' expressions, and only facial expressions showing overt anger or happiness effected trustworthiness scores (negatively and positively respectively) (Engell et al. 2010). People judge the trustworthiness of faces subconsciously, without the opportunity to interact with the individual being judged, and facial trustworthiness characteristics seem similar across cultures (Xu et al. 2012). And, even more importantly, facial trustworthiness seems to predict actual trustworthy and cooperative behaviors in people. In a recent study where a group of subjects were asked to play a prisoners-dilemma type game, and researchers rated the subjects' faces on a scale of trustworthiness, using the characteristics previously published in the Todorov's study (Bonnefon et al. 2017). The results showed that people who had more trustworthy faces, were actually more trustworthy/cooperative during the game (Bonnefon et al. 2017). A similar study was conducted in China using children 8-12 with similar outcomes (Li et al. 2017).

Overall, the majority of previous research used fMRI to determine the extent to which brain regions are used during judgments of trustworthiness, and the earliest studies to examine the ability to judge trustworthiness start at 4 years of age in humans (Ewing et al. 2015b). Given the deficits exhibited by individuals with ASD on assessment of trustworthiness (Li et al. 2017; Ma et al. 2016; Yi et al. 2013b; Yi et al. 2013a) and the need to push for an earlier age of diagnosis of ASD than 2 years of age, it is critical to expand the socioemotional and brain development research to early developmental samples. Furthermore, additional information about the structural changes in the brain regions along social networks responsible for face judgments of trust and other social constructs is needed to understand the neuroanatomical correlates of behavioral changes and alterations throughout primate development. Therefore, this

study aims to characterize early development of facial trustworthiness perception and the underlying neurodevelopmental changes in a highly translational infant *Rhesus macaque* model. We use structural MRI to measure changes in brain structural development of the regions of interest (ROIs) described above (namely: TPO –in the STS-, AMYG, TE, PFC, insula), in parallel to the examination of changes in visual processing of trustworthy and untrustworthy faces (both humans and macaque) in rhesus monkeys ages 1-24 weeks using eye-tracking methods (approximately 1-24 months in humans). The overall hypothesis is that the ability to distinguish between trustworthy and untrustworthy faces won't arise until the end of this developmental period and that this behavior will be correlated with an increase in STS (i.e. TPO), TE, insular and AMY volume. Although children don't become fully capable of judging facial trustworthiness until age 5, the way in which they start judging facial trustworthiness changes significantly during the toddler-preschool years (Ewing et al. 2015b). Even though the children may not know how to properly integrate this information into their social interactions, which may depend on a more mature PFC, they start tracking faces at an adult level early in life (Cogsdill et al. 2014). In rhesus macaques 24 weeks is approximately equivalent to 2 years of age for humans. This time period corresponds to the end of weaning and the infants are spending much more time involved in social interactions with peers and other members of the social group and less with their mothers and families (Reitsema et al. 2016). Due to the similarities in age and social experiences at this time period between monkeys and humans, I expect the macaques to develop the ability to discriminate trustworthy versus untrustworthy faces around 24 weeks of age. Ideally, the results of this study, together with studies in humans, can help inform future human studies and eventually assist in enabling pediatricians to measure changes in eye-tracking and brain MRI as biomarkers for developmental disorders. The study will also hopefully also

contribute to future research into the development of a NHP model for ASD by identifying individual variability and outliers in the development of these social skills and underlying neurocircuits.

Methods:

Subjects

Structural MRI (sMRI) and eye-tracking data were collected longitudinally from 31 male infant rhesus monkeys (*Macaca mulatta);* both sMRI scans and eye-tracking data were collected in 8 subjects, whereas an additional 13 subjects were included in the MRI studies and 10 subjects in the eye-tracking study only (Figure 1). These subjects were housed in outdoor compounds at the Yerkes National Primate Research Center (YNPRC) Field Station (Lawrencville, GA). They lived in large social groups with their mothers and families in order to preserve species-specific social experience. Subject inclusion criteria included: 1) subjects were born to multiparous, competent/nurturing mothers without a history of infant physical abuse or neglect, 2) subjects were from middle-ranking families in the social hierarchy, to control for developmental effects of extreme dominant status, and 3) weighed greater than 450g at birth to avoid the effects of prematurity and low birth weight on brain development (Scott et al. (2016).

Structural MRI

Image Acquisition

Neuroimaging data were collected from a total of 21 infants at 2, 4, 8 12, 16, 20, and 24 weeks of age. Structural MRI scanning sessions took place at the YNPRC Main Center (Atlanta, Georgia.) Each subject was transported with its mother from the Field Station to the Main Center either the day before or the morning of their scheduled scan. The brain MRI scans were acquired using a 3T Siemens Magnetom TRIO system scanner (Siemens Med. Sol., Malvern, PA, USA). High resolution T1-weighted structural MRI scans were collected using a 3D magnetization prepared rapid gradient echo (3D-MPRAGE) parallel imaging sequence (TR/TE = 2600/3.46msec, FoV: 116mm, voxel size: 0.5mm^3 isotropic, 8 averages, GRAPPA, R=2). T2-

weighted MRI scans were collected in the same direction as the T1 images (TR/TE = 3200/373msec, FoV: 128mm, voxel size: 0.5mm^3 isotropic, 3 averages, GRAPPA, R=2) in order to assist in the identification of the brain tissue classes by improving contrast of the borders between grey matter (GM), white matter (WM), and cerebrospinal fluid (CSF), and aid in the delineation of the regions of interest –ROIs- (Knickmeyer et al. 2010). To ensure lack of motion artifacts, subjects were scanned under isoflurane anesthesia (0.8-1% to effect, inhalation) following injection with telazol (2.89±0.60 mg/kg) and intubation. Physiological parameters were monitored throughout the scan using an oximeter, ECG, rectal thermistor, and blood pressure monitor. To maintain normal hydration, an intravenous catheter was used to administer dextrose/NaCl (0.45%). Also, an MRI-compatible heating pad helped maintain the subjects' body temperature throughout the scan. Upon completion of the scans and full recovery from anesthesia, each infant was returned to its mother and the pair returned to their social group on the following day.

Image Processing and Analysis

Structural MRI data were analyzed using AutoSeg (version 3.0.2) and NeoSeg (for some specific steps at the earliest ages: 2 & 4 weeks), software pipelines that automatically segments brain tissue classes, such as GM, WM and CSF, and performs cortical lobar and subcortical parcellations (Wang et al. 2014). In order to do this, AutoSeg uses a 6 step process. First, each subject's scans are corrected for field inhomogeneity through a bias field correction step. MRI machines use radiofrequency coils to transmit radio waves into the section of the body being scanned. Man-made imperfections in the coil result in the image having signal intensity inhomogeneity, or low frequency undesirable signals, which results in gradual variations in the image intensities within the same tissue. AutoSeg employs N4-ITK bias field correction. This

step is necessary in order for the program to perform the segmentation and parcellation steps accurately. Next, the images are registered to a population-based T1-MRI atlas using a reference space algorithm (Wang et al. 2014); (Styner et al. 2007); (Short et al. 2010); (Howell et al. 2014); (Shi et al. 2017). In this study, the UNC-Emory infant rhesus brain atlases were used to register the subjects' images to the atlas closest to their age and grey/white matter signal contrast (Shi et al. 2017). Thus, the 2 and 4 week scans were registered to the 2-week atlas, whereas the 8, 12, and 16 week scans were registered to the 3-month atlas, and the 20 and 24 week scans were registered to the 6-month atlas. To align the subject's image to the atlas image, AutoSeg uses a tool called BRAINSFit (Johnson et al. 2008) for rigid body and affine registration (Wang et al. 2014). Rigid body registration involves 3 rotations and 3 translations, whereas affine registrations also involves 3 scalings and 3 skews/ shears. The third step uses atlas-based classification (ABC) to perform tissue segmentation into GM, WM and CSF tissue classes. ABC segmentation uses signal intensities from both the T1 and the T2 images, and atlas-specific probabilistic tissue priors to assign a label to each voxel. In this study, this step was performed twice, once before skull stripping and once after (Wang et al. 2014). The fourth step is automatic skull stripping, which requires manual quality control and final editing. AutoSeg uses ABC segmentation to separate brain tissue from non-brain tissue (e.g. skull, muscle, vessels) to generate a clean brain image. The fifth step is the single- and multi-atlas-based ROI parcellations, during which AutoSeg uses the ANTS registration tool (Grossman et al. 2008); (Wang et al. 2014) to register each skull-stripped brain atlas image to the skull-stripped subject image. In order to do this, ANTS uses a cross-correlation similarity metric and a symmetric diffeomorphic deformation model to preserve the geometric properties of the subject image even if large distortions are needed for the registration. Then, transformation matrices are generated

for each of the cortical and subcortical parcellations, and these transformations are applied to each region in the atlas to convert them into subject space and generate the subject's parcellations. The tissue class segmentations generated (GM, WM, CSF) are also blended with the cortical parcellations so that the WM, GM, and CSF of each cortical region can be generated. Manual adjustments of the automatic segmentations and parcellations are sometimes necessary to ensure accuracy of the tissue labeling and ROI borders, which we had to apply following published anatomical criteria used in rhesus brain atlases (Paxinos and Mitchell 2000; Saleem 2012). The last step is volume computation of the different tissue classes (WM, GM and CSF), and also for the cortical and subcortical parcellations.

In the present paper, total brain volume was computed as intracranial volume (ICV), which was calculated by the summation of GM, WM, and CSF (including CSF in the subarachnoid space) (see Figure 3a). The ROI volumes calculated in this study were prefrontal cortex (PFC), superior temporal sulcus (STS), inferotemporal cortex (TE), insula, and amygdala (AMY; see Figure 3c and 3d). In order to control for individual variability in brain size, the ROI volumes were corrected for total ICV. The PFC and AMY were defined based on ROIs generated for the UNC-Emory macaque brain atlases (Shi et al. 2017) and all other brain regions were defined using the Paxinos macaque brain atlas (Paxinos and Mitchell 2000). The volume calculated for the PFC included GM, WM, and CSF. During manual editing the PFC was defined using the lateral, dorsal and anterior boundaries marked by the CSF surrounding the brain, the medial boundary marked by the interhemispheric fissure, and the posterior boundary marked by the arcuate sulcus (Knickmeyer et al. 2010). The inferior boundary changed moving rostral to caudal in the brain, defined as the CSF, the sylvian fissure, and the arcuate sulcus (Saleem 2012; Seltzer and Pandya 1978). The temporo-parieto-occipital junction (TPO) region of the STS was

selected for this study. The boundaries of this area were defined medially by the lateral fissure, superiorly by white matter, and inferiorly by the STS (Saleem 2012; Seltzer and Pandya 1978). For the insula, the granular, dysgranular, agranular, and the insular proisocortex subdivisions were all included. The insula was defined medially and superiorly by white matter, and laterally and inferiorly by the lateral sulcus (Saleem 2012; Seltzer and Pandya 1978; Stephani et al. 2011). The anatomical definition of the amygdala used the following boundaries: superior boundary was defined as WM (including the capsule, optic and auditory radiation, and the anterior commissure) and the putamen; posterior inferior boundary was the lateral ventricle/temporal horn and included the amygdala-hippocampal transition area as part of the amygdala ROI; the anterior inferior boundary was the temporal white matter and the entorhinal cortex; the anterior boundary was found at the level where the optic nerves begin to fuse with the optic chiasm and the posterior boundary was the hippocampus; the medial boundary was the meninges, so that the periamygdaloid cortex was included in the amygdala ROI (Knickmeyer et al. 2010; Payne et al. 2010; Saleem 2012). Lastly, area TE was defined by merging TE1, TE2, and TE3. These areas were defined superiorly by the inferior temporal sulcus. Also, lateral and medial boundaries were defined by meninges and WM respectively. The anterior boundary was marked by the beginning of the entorhinal cortex (Knickmeyer et al. 2010; Saleem 2012; Saleem and Tanaka 1996; Suzuki and Amaral 1994).

Eye-tracking Technique

Eye-Tracking Data Acquisition

Eighteen subjects were studied in the eye-tracking portion of this project, following previously published protocols (Muschinski et al. 2016; Parr and Heintz 2009). Briefly, each mother-infant pair were trained to temporarily separate on command from their social group to

be transported to the testing room where the eye-tracking session took place. The mother was anesthetized and were placed in a reclining seat located inside a light and sound attenuated testing chamber, with her awake infant on her ventrum (Figure 2a). Inside the chamber, there was a computer monitor which displayed the visual stimuli, an infrared eye-tracker (ISCAN, 60 Hz), as well as a camera to continuously monitor the mother and infant throughout the testing session, to ensure the safety of the animals and that the infant was paying attention to the stimuli. Within each eye-tracking session the subjects were presented with two separate sets of stimuli: (1) human faces and (2) monkey faces (Figure 2b and 2c). Within each set, there were two faces, one face had trustworthy characteristics and the other had untrustworthy facial characteristics (see definition below, under "Stimuli Selection"). Each eye-tracking session included 2 trials of each stimuli set. To grasp the infant's attention cartoons and nature videos were projected on the computer monitor, then individual calibration points were presented at 5 different locations on the screen. Following calibration, the stimuli were presented to each infant, randomized individually for each testing session. The infants' looking behavior was recorded to extract time looking at either the trustworthy or untrustworthy face, and within each face, to measure the amount of time spent looking at each facial feature (eye region, mouth region, and total face region) which were defined as separate regions of interest (ROIs) in the images by trained coders (see Figure 2c). The eye region was defined as the eyeball, eyebrow, and orbicularis oculi muscle, the mouth was defined as the lips and the orbicularis oris muscle, and the total face included the mouth, eyes, nose, forehead, and cheeks (everything except ears and neck) (see Figure 2c). GazeTracker, a computer software, computes the fixations using three parameters, sample number (acquired at 60 Hz), duration (in ms), and spatial location (diameter in pixels). Each video recording from each session were examined to verify that the infants paid attention to

the stimuli when the infrared device registered that they were (i.e.: the infants were not just moving their heads around with occasional glimpses being picked up by the tracker).

Stimuli Selection

The trustworthy and untrustworthy monkey and human faces were generated based on previous research about human trustworthy facial features. The human faces came from a well-studied bank of faces created by Alexander Todorov and his group (Todorov et al. 2008) based on previous studies showing that trustworthy facial features include: high inner eyebrows, wide eyes, pronounced cheekbones, wide chins, and shallow nose sellion. In contrast, untrustworthy facial features involve: low inner eyebrows, narrow eyes, shallow cheekbones, thin chins, and deep nose sellion (Todorov et al. 2008). The monkey faces were selected from a database of pictures taken from macaques living in social groups at the YNPRC Field Station that consisted of natural facial expressions modeling similar trustworthy and untrustworthy facial features as described for humans. No previous research has been done to identify trustworthy and untrustworthy facial features in *Rhesus macaques*, and future studies would be needed to validate the ethological relevance of facial features selected in this study in relation to trustworthiness in this species.

Statistical Analysis

sMRI Data

Repeated Measures Analysis of Variances (rmANOVA) was used to analyze the ICV and volumetric ROI data, with AGE (2, 4, 8, 12, 16, 20, 24 weeks) and HEMISPHERE (left vs right) as repeated, within-subject factors. Data from 19 of the 21 animals was included in this analysis; the two animals excluded had missing data from multiple scan dates. Due to the age-related increases in ICV reported in results, an additional rmANOVA's was conducted to analyze the

developmental changes in regional volumes after ICV-correction. These statistical models were built using IBM SPSS Statistics (IBM Corporation, Armonk, NY). Whenever a main or interaction effect was detected, a Bonferroni pairwise multiple comparison was conducted. All results where $p \leq 0.05$ were considered significant and all results where $0.06 < p < 0.1$ were considered as statistical trend.

Eye-Tracking Data

Due to the small sample size of the study and intrinsic difficulty of eye-tracking studies in freely-behaving infant macaques, a large amount of data was missing from the eye-tracking sessions. This challenged the use of a rmANOVA to analyze all subjects' longitudinal data, and the use of boot-strapping methods to fill in the missing data was also inappropriate because much more than 5% of the data was missing. Thus, in addition to presenting the plots of the full set of individual eye-tracking data, to show the group developmental patterns as well as individual variability data, I am also presenting some statistical analyses done following two methods. First, I present the descriptive statistics to show the mean and standard error of the mean at each time point for the preference for faces over the background (Microsoft Excel (Microsoft, Redmond, WA) was used to create bar graphs to aid in the description of these results). Second, I used rmANOVA to analyze percent fixation on facial features for a subset of subjects at a specific subset of ages with the maximum data. Thus, results of human face stimuli analyses included data from 5 subjects from sessions that took place at 5, 9, and 21 weeks of age. For the monkey face stimuli analysis, data from 6 subjects was included from sessions that took place at 5, 9, and 23 weeks of age. For both sets of stimuli, two rmANOVAs were conducted, one analyzing the percent of time looking at each facial feature (eyes, mouth, and whole face) over the total time looking at the stimulus, and another analyzing the percent of time looking at the eyes and nose

over the time subjects spent looking at the whole face. For both rmANOVAs, AGE (5, 9, 21, 23) and STIMULI TYPE (trustworthy vs untrustworthy) were used as the repeated factors. All results where $p \leq 0.05$ were considered significant and all results where $0.06 < p < 0.1$ were considered statistical trends.

Results

Structural MRI Data

Absolute Volumes

Total Intracranial Volume (ICV)

Analysis of total ICV revealed a significant main effect of AGE ($F(6,108)=667.315$, $p < 0.0005$, $\eta2=0.974$; Figure 4a). Bonferroni pairwise comparisons showed that ICV continuously increased from 2 weeks of age to 23 weeks of age with significant increases in volume between each age points ($p<0.02$). As seen in Figure 4b, the average whole brain GM, WM, and CSF had similar trajectories to ICV.

Total Prefrontal Cortex (PFC) Volume

Analysis of total PFC volume revealed a significant main effect of AGE ($F(6,108)=531.114$, $p < 0.01$, $\eta2=0.969$; Figure 5). However, there was no main effect of HEMISPHERE($F(1,18)=.771$, $p = 0.391$, $\eta2=.041$), and no interaction effect of AGE by HEMISPHERE ($F(6,108)=1.686$, $p=0.131$, $\eta2=0.086$). The Bonferroni pairwise comparisons performed for the AGE main effect showed significant increases in PFC volume from 2 to 24 weeks of age with significant ($p < 0.01$) except for plateaus in growth from 12-16 weeks of age ($p=0.260$) and from 20-24weeks of age ($p=0.403$).

Temporo-Parieto-Occipital (TPO) Junction Volume

TPO volume was identified to have a significant main effects of AGE ($F(6,108)=1045.332$, $p < 0.0005$, $\eta2=0.983$: Figure 6), HEMISPHERE ($F(1,18)=419.919$, $p < 0.0005$, $\eta2=0.959$), and an interaction effect of AGE by HEMISPHERE ($F(6,108)=87.445$, $p < 0.01$, $\eta2=0.829$). The post-hoc pairwise comparisons for the AGE effect revealed that the TPO grew continuously from 2 weeks to 23 weeks of age ($p < 0.01$ in all comparisons).

Inferotemporal Cortex (TE) Volume

Analysis of TE volume revealed significant main effects of AGE ($F(6,108)=660.691$, $p < 0.01$, $\eta 2=0.973$; Figure 7), HEMISPHERE ($F(1,18)=16.569$, $p=0.001$, $\eta 2=0.479$), and an AGE by HEMISPHERE interaction effect ($F(6,108)=8.573$, $p < 0.01$, $\eta 2=0.323$). The Bonferroni pairwise comparisons of the AGE main effect revealed that the TE grew from 2 weeks to 23 weeks of age, with the rate of growth slowing from 8 weeks to 16 weeks of age (8-12 weeks $p=0.11$, 8-16weeks $p=0.123$, 12-16 weeks $p=1$) and 20-24 weeks of age ($p=0.306$). Increases in volume between all other ages were significant ($p < 0.05$).

Insula Volume

It was identified that insula volume had a significant main effect. ($F(6,108)=224$, $p < 0.01$, $\eta 2=0.953$: Figure 8) and HEMISPHERE ($F(1,18)=7.428$ $p = 0.014$, $\eta 2=0.292$), as well as a significant AGE by HEMISPHERE effect ($F(6,108)=57.670$ $p < 0.01$, $\eta 2=0.762$). The Bonferroni pairwise comparisons of the AGE main effect revealed that the insula grew from 2 weeks to 23 weeks of age with a plateau in growth from 8-16 weeks of age (8-12 weeks $p= 0.82$, 12-16 weeks $p=0.877$) and 20-24 weeks of age ($p=1$). Increases in volume between all other ages were significant ($p<0.05$).

Amygdala (AMY) Volume

Analysis of AMY volume revealed significant main effects of AGE ($F(6,108)=363.474$, $p < 0.01$, $\eta 2=0.953$; Figure 9), HEMISPHERE $F(1,18)=5.187$ $p = 0.036$, $\eta 2=.234$) and an interaction effect of AGE by HEMISPHERE ($F(6,108)=11.245$, $p < 0.01$, $\eta 2=0.398$). Bonferroni pairwise comparisons of the AGE main effect revealed that the AMY grew from 2 weeks to 23 weeks of age with slowing in the rate of growth from 8 weeks to 16 weeks of age (8-12 weeks p=

1, 8-16weeks p=0.296, 12-16 weeks p=1) and 20-24 weeks of age (p=0.306). Increases in volume between all other ages were significant (p<0.05.

ICV-Corrected Brain Regional Volumes

Because ICV showed a significant increase with age, each brain region's volume was ICV-corrected to take ICV into consideration. This was done by calculating the percent of each ROI volume over ICV.

ICV-Corrected Prefrontal Cortex (PFC) Volume:

When analyzing the percent change in PFC volume over the total ICV change (Figure 10), there was a significant main effect of AGE ($F(6, 108)=10.186$, $p < 0.01$); however there was no main effect of HEMISPHERE ($F(1, 18)= 0.827$, $p =0.375$) nor an interaction effect of AGE by HEMISPHERE ($F(6, 108)=1.865$, $p =0.093$). As the Bonferroni multiple comparison of the AGE main effect revealed, there was an increase in volume of the PFC from 2-24 weeks of age ($p<0.01$), however with the exception of significant growth from 2 to 4 weeks of age ($p<0.01$) there was no growth between consecutive ages during the entire time period ($p=1.00$) Overall, the PFC increased at a similar rate as ICV.

ICV-Corrected Temporo-Parieto-Occipital (TPO) Volume:

When analyzing the percent change in TPO volume over ICV (ICV-corrected TPO volume, Figure 11), there were main effects of AGE ($F(6, 108)= 1529.332$, $p < 0.01$), HEMISPHERE ($F(1, 18)=442.082$, $p < 0.01$), and a significant AGE by HEMISPHERE interaction effect ($F(6, 108)=217.159$, $p < 0.01$). Results of the Bonferroni pairwise comparison of the AGE main effect revealed that the TPO grew from 2 to 24 weeks of age ($p<0.05$) with the exception of minimal growth from 8-16 weeks of age and 20-24 weeks of age (8-12 weeks p=1.00, 12-1 6weeks p=1.00, 8-16 weeks p=1.00, and 20-24 weeks p=.109). In the left

hemisphere the TPO grows at a faster rate than ICV throughout the developmental period, whereas the TPO in right hemisphere increases volume at the same rate as ICV until 12 weeks of age and then begins to grow rapidly.

ICV-Corrected Inferotemporal Cortex (TE) Volume:

When analyzing the percent change in TE volume over ICV (Figure 12), there were main effects of AGE ($F(6,108)=959.382$, $p < 0.01$), HEMISPHERE ($F(1,18)=20.901$, $p < 0.01$), and an interaction effect of AGE by HEMISPHERE ($F(6,108)=15.824$, $p < 0.001$). A Bonferroni pairwise comparison of the AGE main effect revealed that area TE increased in volume over the period of study ($p<0.01$), however, there was minimal growth from 2 to 4 weeks of age ($p=0.996$), and a plateau in growth from 8-16 weeks of age and 20-24 weeks of age (8-12 weeks $p=1.00$, 12-16weeks $p=1.00$, 8-16 weeks $p=1.00$, and 20-24 weeks $p=1.00$). Both hemispheres of the TE increase in volume at faster rate than ICV.

ICV-Corrected Insula Volume:

When analyzing the percent change in insula volume over ICV (Figure 13), there were main effects of AGE ($F(6, 108)=99.317$, $p < 0.01$), HEMISPHERE ($F(1, 18)= 7.535$, $p = 0.013$), and an interaction effect of AGE by HEMISPHERE ($F(6, 108)=54.005$, $p < 0.01$). A Bonferroni pairwise comparison of the AGE main effect revealed there was an increase in volume of the insula from 2 to 24 weeks of age ($p < 0.05$), however there was minimal growth from 20-24 weeks of age ($p=1.00$) and no difference in volume at 2 weeks of age and 8 weeks of age ($p=1.00$). In both hemispheres, the insula increases in volume at a similar rate to ICV until 20 weeks of age, where they start to increase in the rate of growth; however, from 20 to 24 weeks of age the insula in the right hemisphere begins to grow at a faster rate than that of the left hemisphere.

ICV-Corrected Amygdala(AMY) Volume:

When analyzing the percent change in amygdala volume over ICV (Figure 14), main effects were identified for AGE ($F(6, 108)=201.909$, $p < 0.01$), HEMISPHERE ($F(1, 18)= 3.222$, $p =0.011$), and an interaction effect of AGE by HEMISPHERE ($F(6, 108)=11.981$, $p < 0.01$). A Bonferroni pairwise comparison of the AGE main effect revealed that there was an increase in AMY volume relative to ICV from 2 to 24 weeks of age, however there was no growth from 2-4 weeks of age (p=1.00), 8-16 weeks of age (8-12 weeks p=0.066, 12-16 weeks p=1.00) and 20-24 weeks of age (p=1.00). In both hemispheres, the amygdala increases in volume at a faster rate than ICV for the first 8 weeks, then they start to grow at a similar rate to ICV.

Eye-Tracking Data

Human Faces

Faces vs Background

As seen in Figure 15, from 3 to 23 weeks of age, the subjects show increased preference for looking at human faces over the background of the presented stimuli. Starting at 3 weeks of age the error bars depicting the standard error of the mean no longer overlap, and the value for percent time of fixation is higher for faces than for the background. Table 1 shows the values for the average percent looking time at human faces and the background of the stimuli for each age.

Percent time looking at facial features over total time looking at stimuli

Eyes

The graph of the raw data for all the subjects (Figure 16) shows that percent time looking at the trustworthy eyes with age increased from 2-8 weeks of age, decreased from 8-17 weeks of age, and then increased from 17-24 weeks of age. This was similar to the pattern of percent time

looking at the untrustworthy eyes with age; however, for the untrustworthy eyes, the percent looking time remained constant from 17-24 weeks of age. Analysis of the percent time spent looking at the eyes over total stimulus time for 5 subjects at 3 ages revealed no significant main effects of AGE ($F(2, 8)=.858$, $p = 0.460$, $\eta2=0.177$), STIMULI TYPE ($F(1,4)=1.558$ $p =.280$, $\eta2=0.280$), nor an interaction effect of AGE by STIMULI TYPE ($F(2, 8)=1.115$ $p=0.374$, $\eta2=0.218$).

Mouth

The graph of the raw data for all the subjects (Figure 17) shows a similar overall trend of percent time looking at the trustworthy and untrustworthy mouth with age. This trend is a decrease in looking time from 2 to 11 weeks of age and then a slight increase in looking time that stabilizes up to 24 weeks. Analysis of the percentage of time spent looking at the mouth in comparison to the total stimulus time for 5 subjects at 3 ages revealed no significant main effects of AGE ($F(2, 8)=.287$, $p =0.758$, $\eta2=0.067$), STIMULI TYPE ($F(1,4)=1.110$ $p =.352$, $\eta2=0.217$), nor the interaction of AGE by STIMULI TYPE ($F(2, 8)=.351$ $p=0.714$, $\eta2=0.081$).

Total Face

The graph of the raw data for all the subjects (Figure 18 a) shows different pattern for the percent time looking at the trustworthy and untrustworthy faces with age. For the trustworthy face there is an increase in looking time from 2-6 weeks of age, followed by a decrease in looking time from 6-17 weeks of age, and then an increase in looking time from 17-24 weeks of age. For the untrustworthy face there is an increase in looking time from 2-15 weeks of age, and then a decrease in looking time from 15-24 weeks of age. Analysis of the percentage of time spent looking at faces for 5 subjects at 3 ages revealed a significant main effect of AGE ($F(2, 8)=6.464$, $p =0.021$, $\eta2=0.618$; Figure 18 b). The Bonferroni pairwise comparison analysis

revealed a trend (p=0.086) towards decreasing looking time from 5 weeks to 9 weeks of age, and then a significant (p=0.009) increase in looking time from 9 weeks to 21 weeks of age. However, there was no significant (p= 0.505) change in looking time from 5 weeks to 21 weeks of age. Furthermore, there was no significant main effect of STIMULI TYPE ($F(1,4)=0.057$ $p=0.823$, $\eta2=0.057$) and no interaction effect of AGE by STIMULI TYPE ($F(2, 8)=0.637$ $p=0.554$, $\eta2=0.137$).

Percent looking time at facial features over time looking at the whole face

Eyes

The graph of the raw data for all the subjects (Figure 19 a) shows an overall trend of percent time looking at the trustworthy eyes in relation to total face with age increased from 2-6 weeks of age, then decreased from 6-17 weeks of age, and then increased from 17-24 weeks of age. The trend for percent looking time at the untrustworthy eyes in relation to total face with age was the opposite, with a decrease in looking time from 2-6 weeks of age, an increase in looking time from 6-17 weeks of age, and then a decrease in looking time from 17-24 weeks of age. Analysis of the percent time subjects spent looking at the eyes in comparison to the whole face for 5 subjects at 3 ages revealed no main effects of AGE ($F(2, 8)=.045$, $p=0.815$, $\eta2=.050$), STIMULI TYPE ($F(1,4)=0.865$, $p=0.405$, $\eta2=0.178$), nor AGE by STIMULI TYPE($F(2, 8)=1.25$ $p=0.337$, $\eta2=.238$).

Mouth

The graph of the raw data for all the subjects (Figure 20) shows a similar overall trend of percent time looking at the trustworthy and untrustworthy mouth in relation to face with age. This is a decrease in looking time from 2 to 11 weeks of age and then a slight increase in looking time that stabilizes up to 24 weeks. Analysis of the percentage of time spent looking at the mouth

compared to time looking at the face for 5 subjects at 3 ages revealed no significant main effects of AGE ($F(2, 8)=2.007$, $p = 0.197$ $\eta2=0.334$), STIMULI TYPE ($F(1,4)=0.75$, $p =0.798$, $\eta2=.018$), nor an interaction effect of AGE by STIMULI TYPE ($F(2, 8)=1.930$, $p=0.207$, $\eta2=0.325$).

Monkey Faces

Faces vs Background

As seen in Figure 21, from 3 weeks to 23 weeks of age, the subjects show a likely significant preference for looking at monkey faces over the background of the stimuli presented on the screen. Starting at 3 weeks of age the error bars depicting the standard error of the mean do not overlap, and the value for percent time of fixation is higher for faces than for the background. Table 2 shows the values for the average percent looking time at monkey faces and the background of the stimuli for each age.

Percent time looking at facial features over total time looking at stimuli

Eyes

The graph of the raw data for all the subjects (Figure 22) shows an overall trend of constant percent looking time at the trustworthy and untrustworthy eyes with age. Analysis of the percent time spent looking at the eyes for 6 subjects at 3 ages revealed no significant main effects of AGE ($F(2, 10)=.045$ $p =0.956$, $\eta2=0.009$), STIMULI TYPE ($F(1,5)=2.451$, $p =.178$, $\eta2=.329$), or an interaction effect of AGE by STIMULI TYPE ($F(2, 10)=0.583$, $p=0.576$, $\eta2=.104$).

Mouth

The graph of the raw data for all the subjects (Figure 23 a) shows an overall trend of increased percent looking time at the trustworthy and untrustworthy mouths with age. Analysis

of the percent time spent looking at the mouth for 6 subjects at 3 ages revealed a significant main effects of AGE ($F(2, 10)=4.088$, $p =0.05$, $\eta 2=0.450$; Figure 23 b), with the amount of time spent looking at the mouth increasing from 5 weeks to 23 weeks of age. There were no significant main effects of STIMULI TYPE ($F(1,5)=.115$, $p =.748$, $\eta 2=0.022$), and no interaction effect of AGE by STIMULI TYPE ($F(2, 10)=0.106$, $p=0.900$, $\eta 2=0.021$).

Face

The graph of the raw data for all the subjects (Figure 24) shows different patterns for the percent time looking at the trustworthy and untrustworthy faces with age. For the trustworthy face there is an increase in looking time from 2-17 weeks of age, then a decrease in looking time from 17-24 weeks of age. For the untrustworthy face there is an increase in looking time from 2-6 weeks of age, then a decrease in looking time from 6-17 weeks of age, and then an increase in looking time from 17-24 weeks of age. Analysis of the percent time spent looking at faces for 6 subjects at 3 ages revealed no significant main effects of AGE ($F(2, 10)=1.437$ $p =0.283$, $\eta 2=0.223$), STIMULI TYPE ($F(1,5)=0.417$ $p =.547$, $\eta 2=0.077$, $\eta 2=0.329$), and no interaction effect of AGE by STIMULI TYPE ($F(2, 10)=0.612$ $p=0.561$, $\eta 2=0.104$).

Percent looking time at facial features over time looking at the whole face

Eyes

The graph of the raw data for all the subjects (Figure 25 a) shows an overall trend of increased percent looking time at the trustworthy eyes in relation to face with age. For the untrustworthy eyes, there is an increase in percent looking time from 2-17 weeks and then a decrease from 17-24 weeks. Analysis of the percentage of time spent looking at the eyes when the subject was looking at a face for 6 subjects at 3 ages revealed a significant no main effect of

AGE ($F(2, 10)=.378$ $p =0.697$, $\eta 2=.086$), STIMULI TYPE ($F(1,5)=0.055$, $p =0.826$, $\eta 2=0.014$), nor an interaction effect of AGE by STIMULI TYPE ($F(2, 10)=0.196$, $p=.826$, $\eta 2=.047$).

Mouth

The graph of the raw data for all the subjects (Figure 26 a) shows an overall trend of increased percent looking time at the trustworthy and untrustworthy mouths with age. Analysis of the percentage of time spent looking at the mouth in comparison to time looking at the face revealed a significant main effect of AGE ($F(2, 10)=5.245$, $p =0.028$, $\eta 2=0.512$; Figure 26 b), with the amount of time spent looking at the mouth increasing from 5 weeks to 23 weeks of age. There was no significant main effect of STIMULI TYPE ($F(1,5)=.2.673$, $p =0.163$, $\eta 2=0.348$), and no interaction effect of AGE by STIMULI TYPE ($F(2, 10)=1.078$, $p=0.377$, $\eta 2=0.177$).

Discussion:

The main goal of this study was to characterize the early development of socio-visual engagement in infant rhesus monkeys, specifically perception of trustworthy and untrustworthy facial features, and examine the underlying neurodevelopmental changes in the structure of brain regions involved in this ability (PFC, STS, TE, insula, AMY) along social networks. To accomplish this, structural MRI scans and eye-tracking data were collected to examine how the infants scanned facial features of monkeys and humans during their first 24 weeks of life. The results of the sMRI study show that all the studied ROIs significantly increased in volume from 2 to 24 weeks of age, although they showed region specific developmental trajectory patterns. There were also strong laterality effects in most of the brain regions, except for the PFC, which showed similar volumetric changes across ages in both the left and right hemispheres. Also, all the ROIs except the TPO showed a significant slowing in growth around 12 weeks of age. Now, because ICV -the measure used here to calculate volumetric brain changes, which includes GM, WM and CSF- increased with age, the ROI volumes growths were also analyzed after ICV correction. Even when correcting for ICV growth, most ROIs, except for the PFC, maintained a significant volume growth with age, suggesting that the growth detected in the ROIs are region-specific and not just tracking overall general increases in brain size. The eye-tracking results show that infants had a preference for both human and monkey faces over stimulus background that emerged at 3 weeks of age. There was a unique "U-shaped" pattern when viewing human faces where they spent more time looking at faces at 5 and 21 weeks of age than they did at 9 weeks. The results also revealed that for both human and monkey stimuli, when the subjects were looking at the faces, they spent more time looking at the untrustworthy eyes than at the trustworthy eyes. Finally, the results showed that when viewing the monkey stimuli, the subjects

increased the time looking at the mouth with age, in relation to total time and time looking at just the faces. Altogether, the findings from this study suggest that the face processing regions of the primate brain have rapid and distinct growth trajectories during the infant period, which that take place in parallel to developmental changes in the unique way infant macaques view and process faces (See Table 3 for a summary of these findings).

Brain Regions

The ICV increased drastically from 2 to 12 weeks of age, followed by a slowed rate of growth from 12 to 24 weeks of age. Other NHP studies have reported similar results, with total brain volume (TBV) increasing rapidly from birth through 12 weeks of age and then continuing to grow but at a slower rate from 12 to 24 weeks (Liu et al. 2015; Malkova et al. 2006). These studies are different from our study in that they defined TBV as GM+WM rather than ICV (GM+WM+CSF). We chose to use ICV rather TBV because (1) it included ventricles and CSF as components of the central nervous system that show significant growth and play an important role during development and (2) controlled for any mislabeling in the tissue classification process of GM or WM as CSF. Despite the difference in calculation, TBV and ICV are both accepted values for whole brain size, and the similarity in growth trajectories across different infant macaque studies suggests that CSF volume increases in a similar way to GM and WM tissue volumes, as shown by our findings (see Figures 4b). This means that CSF volume changes are not driving the overall brain volume (ICV) changes. Studies in human infants show similar results, with humans showing rapid growth occurring from birth to one year of age (equivalent to approximately 12 weeks in monkeys), followed by slowed growth from 1 to 2 years (similar to 24 weeks in monkeys) (Giedd et al. 2009; Knickmeyer et al. 2008; Knickmeyer et al. 2010; Liu et al. 2015; Malkova et al. 2006). There are also some differences in postnatal brain growth

between humans and macaques. The biggest difference being that there is less postnatal brain growth in macaques than in humans, with macaque brain size increasing by 50% over the first year of life, while humans' increase by 100% over the same developmental period (Hill et al. 2010; Liu et al. 2015; Malkova et al. 2006). Despite this difference the pattern of the developmental trajectories of brain volume growth are very similar during this time period. What biological mechanisms underlie these developmental brain volume increases in primates? In macaques, cortical neurogenesis is nearly complete by the beginning of the third trimester of gestation, and therefore does not contribute to the observed postnatal volume growth, except for a few brain regions that maintain neurogenesis through adulthood, such as the hippocampus (Bourgeois et al. 1994; Bourgeois and Rakic 1993; Scott et al. 2016; Zecevic 1998). However, postnatal dendritic arborization and synaptic density increases significantly after birth, and may be one of the contributing factors to the increases in postnatal brain volume (Bourgeois et al. 1994; Bourgeois and Rakic 1993; Scott et al. 2016; Zecevic 1998). Previous studies show that synaptogenesis in macaques rapidly increases from birth to 2 months of age throughout the brain, although with some region-specific differences in growth rate with age (Scott et al. 2016). As the monkey infant transitions into the juvenile period (1-3 years) and then into adolescence (3-5 years), synaptic pruning begins to occur and slight decreases in the volume of some brain regions are observed (Scott et al. 2016). Altogether, both humans and primates undergo rapid increases in postnatal brain growth that lead to a prolonged period of sensitivity to social environment as well as to interventions.

The PFC growth trajectory showed a similar growth pattern to ICV, suggesting that the increases in PFC volume track along the general increases in total brain size during this infant developmental time and may not be region-specific. In general, the rate of change of the PFC

volume during infancy was much slower than that of the other brain regions in the study. This is similar to previous reports showing that the PFC grows slower than other regions of the brain during the infant and juvenile periods, especially when compared with those involved in sensory processing in both humans (Giedd and Rapoport 2010; Gogtay et al. 2004) and nonhuman primates (Malkova et al. 2006). It has to be noted that our study focused on total PFC volume growth, which is different from reports of PFC WM growth in primates (Matsuzawa et al. 2001). The PFC plays an important role in executive function, including attention, working memory, decision making, goal-directed behavior, impulse control, as well as on social, emotional and stress regulation (Barbas and Zikopoulos 2007; Machado and Bachevalier 2003), which are all skills that mature later in life and are not fully developed during infancy. Functionally the PFC shows a protracted maturation that parallels its slow structural development through adolescence and until early adulthood (Giedd et al. 2009; Giedd and Rapoport 2010; Gogtay et al. 2004; Tarullo and Gunnar 2006; Thompson-Schill et al. 2009). This slow growth rate exposes the PFC to a long period of sensitivity during development where damage to the region can have major effects on behavioral and cognitive function, and, conversely, adverse life experience can have large effects on the PFC's development. Many disorders have been associated with changes in PFC structure, function, and connectivity during childhood and adolescence, such as schizophrenia, depression, anxiety, ASD, and attention deficit hyperactive disorder (ADHD). Specifically, adults with ADHD have a significantly more symmetrical PFC (GM and WM) than typically developing adults, with differences in asymmetry emerging between the two groups at as early as age 5 (Castellanos et al. 2001; Castellanos et al. 1996). Previous work shows that symmetry in the PFC is typical during the first 6 months of life in humans (Gilmore et al. 2012; Scott et al. 2016), and our study confirms that this is also true for macaques with no laterality

effect being detected in the analysis of PFC growth from 2 to 24 weeks of age. However, in typically developing individuals asymmetry gradually increases with age (Gilmore et al. 2012; Scott et al. 2016). Thus, the time period where PFC switches from symmetric to asymmetric in typically developing children could represent a critical period in development. This could be when brain structure changes from being typical to atypical in neurodevelopmental disorders like ADHD or ASD and open for early intervention. Another interesting finding from the PFC results was the high individual variability not only in absolute volume of the PFC, but also in its growth trajectory in relation to ICV growth. The subjects seem clustered into three different growth patterns, a cluster showing early rapid growth in comparison to ICV, another cluster of animals showing initial slow PFC growth in comparison to ICV that accelerates towards the later ages, and a third cluster maintaining the same growth rate as the ICV from 2-24 weeks. Individual differences in PFC development and growth trajectories have been linked to genetic and early environment factors, such as caregiving received, juvenile play, and social network size (Kolb et al. 2012; Sallet et al. 2011). Although no information is available to address any of these potential factors in our study, future studies are needed to examine the mechanisms that can explain the large individual variability in PFC developmental patterns as well as its functional correlates.

The TPO also showed significant growth from 2 to 24 weeks of age, even after ICV correction. Inspection of the slope of the graph that shows the ratio of TPO volume versus ICV (Figure 10) illustrates that the TPO, especially in the right hemisphere, is growing faster than the rest of the brain (as represented by the ICV corrected ratios), and the growth accelerates even more after 12 weeks of age. This fast growth pattern has also been reported in human infant structural MRI studies, where the TPO grows at a slow rate from birth to age 1, and then grows

more rapidly from 1 to 2 years (Gilmore et al., 2011). The accelerated development at the later ages could be related to the TPO's role and recruitment during more complicated social tasks as the individuals mature (Schobert et al. 2018). Supporting this hypothesis is evidence showing that TPO size is associated with social network size and social skill abilities in both macaques and humans (Sallet et al. 2011). This suggests that not only would the TPO be growing rapidly during infancy to learn and prepare infant macaques for their future complex social interactions, but during weaning the infants would be expanding their social network size from just their mother and family members to increasingly intense and complex social interactions with peers and other animals in their troop, which could be facilitating TPOs growth (Dettmer et al. 2016a; Ferrari et al. 2009; Suomi 2005a, b). There is also evidence of associations between GM volume of the TPO and social rank, with the large TPO volumes in dominant macaques (Sallet et al. 2011). It has been suggested that the STS/TPO is modulating, and being modulated by, social experiences and is needed early on to navigate the relationships involved in social hierarchy (Noonan et al. 2005; Sallet et al. 2011; Utevsky and Platt 2014). The STS is involved in imitation behavior in response to the sight of action in others, specifically in imitation of facial expressions (Heimann 1989; Molenberghs et al. 2010). In macaques, facial expression imitation abilities during infancy can predict future social skill competencies (Kaburu et al. 2016; Meltzoff and Moore 1992). Due to the importance of facial expressions in macaque communication (Parr and Heintz 2009; Parr et al. 2006), learning the proper expressions to make and when to make them is key to interacting with the social world. In both rhesus macaques and humans there are large individual differences in how well infants imitate those around them (Heimann 1989; Molenberghs et al. 2010). It's been found that in rhesus macaques, neonatal imitators look more at faces, especially at the eye region of conspecifics by 10-28 days old, and they are

better at gaze following by 7 months of age than non–imitators (Heimann 1989; Kaburu et al. 2016). This suggests that imitators may process social cues more efficiently. Furthermore, previous work has shown that by the first week of life additional differences between imitators and non-imitators exist, with imitators remembering more social partners, being more attentive during imitation assessments, and exhibiting better delayed imitation (Kaburu et al. 2016; Meltzoff and Moore 1992). All these skills suggest that imitators may mature socially earlier than non-imitators. Similar social implications of imitation skills are also found in human infants. Studies have shown that newborns are able to imitate open mouth and tongue protrusion gestures, as well as facial expressions (Meltzoff and Moore 1977, 1992). An interpretation of the role of this behavior is that neonatal imitation enriches the infant's social ability and strengthens its bond with caregivers (Bjorklund 1987). The importance of facial expression imitation in social development suggests that the STS may grow rapidly in comparison to other brain areas from 2 to 24 weeks of life in macaques to facilitate their ability to imitate facial expressions and develop the skills for healthy social interactions necessary for the weaning period. Interestingly, there are also facial expression imitation differences between typically developing children and those with ASD. An experiment conducted with preschool aged children showed that in comparison to typically developing children, children with ASD engaged less in the imitation of action with objects, and had more difficulty imitating facial expressions (Markodimitraki et al. 2012). The role of the STS in facial expression imitation suggests that further investigation into its link with ASD might help better understand the etiology of ASD.

The growth trajectory of the insula's absolute volume showed increase in volume from 2-8 weeks of age, with a plateau in growth from 8-16 weeks, followed by increases in volume

again from 16-24 weeks of age. Also, similar to the PFC, the insula showed a flat growth rate after ICV correction, suggesting that the increase in insula volume followed global patterns of overall brain growth. Consistent with our findings, a previous developmental structural MRI study in macaques also reported similar, somewhat flat, insula volume growth trajectory, with only a 30% volume increase in the first 5 years of life (Scott et al. 2016). Interestingly, results in macaques show a different growth trajectory for the insula than those seen in humans at similar developmental period ages, where the insula is considered one of the fastest growing regions during infancy (Gilmore et al. 2012). The species differences in growth rate could be explained by overall comparative differences in insula volume, with humans having a larger insula than macaques proportionally to total brain volume (Hill et al. 2010; Shaw et al. 2008). Previous studies have shown that the insular cortex displays a moderate amount of "evolutionary expansion" between macaques and humans, with the occipital lobe showing the least and the frontal lobe showing the most expansion (Hill et al. 2010). In humans, the insula has been associated with interoceptive or visceral sensations, pain, body movement, emotions, vocalizations, internal awareness, and consciousness (Augustine 1996; Craig 2009; Gilmore et al. 2012; Nagai et al. 2007). In macaques, there is evidence for similarities in insula function, with somatosensory and auditory representation in the posterior insula and visceral and automatic functions in the anterior insula (Augustine 1996), and even the cytoarchitecture of the insula is similar in macaques and humans, with insula-unique Von Economo neurons existing in both humans and macaques (Evrard et al. 2012). Thus, the insula may grow early on in order to equip monkeys and humans with integration of internal and external information to adapt to the world they increasingly explore during weaning and pre-school years respectively. A developed insula would enable them to communicate their needs in emergencies through vocalizations and

when to retreat due to injury (Boly et al. 2013; Parr et al. 2006).

In contrast to the other ROIs in this study, area TE showed rapid growth from 2 to 24 weeks of age, even after ICV correction, suggesting a fast-growing trajectory that is region-specific. In humans the fusiform gyrus (the anatomical correlate to area TE in macaques) is also considered to be one of the fastest growing regions during infancy and juvenile periods (Gilmore et al. 2012). The growth trajectory of TE found in this study is similar to that found in human infant structural MRI studies (Gilmore et al. 2012; Gogtay et al. 2004). The results show that TE volume increases faster than ICV during the first 24 weeks of infancy. Area TE is highly involved in face recognition and is thought to develop early due to its important functional role in social interactions (Ungerleider et al. 1998); also, it is in close proximity to the auditory and visual cortices that are known to grow at a faster rate early in development than other areas of the brain (Bartels and Zeki 2000; Gogtay et al. 2004; Kanwisher and Yovel 2006). Since at 12 weeks of age weaning has started, it is important for area TE to grow early in development. Previous fMRI work shows that the face patch of the inferotemporal cortex emerges at 200 days (28-29 weeks) in macaques, but that foveal biases are detected in neonates (Tsao et al. 2008). This implies that functionally, TE is developing the underlying connections that allows it to be a face specific region later in development. During the weaning period, infant macaques begin to make more reciprocal eye-contact and face-to-face interactions with their mother and with their family members and peers for the first time (Dettmer et al. 2016a; Ferrari et al. 2009; Suomi 2005b). Thus, early development of the TE can assist in the macaque's ability to be prepared for this time period, but then once weaning begins around 12 weeks of age, the increased amount of face-to face interactions could facilitate TE growth.

The results for the amygdala's volume growth trajectory in this study are also consistent with previous research. The amygdala grows rapidly from 2 to 12 weeks of age, followed by slower growth rate from 12 to 24 weeks. The early and late ages amygdala absolute volumes also align with results from previous research (Payne et al. 2010) showing that the volume of the amygdala in each hemisphere is about 100 mm^3 at 2 weeks of age and doubled to about 200 mm^3 at 24 weeks. Similar growth trajectories have also been reported in human infants, with rapid growth of the amygdala in the first year of life, and slowing down from 1 to 2 years of age (Uematsu et al. 2012). The amygdala maintained the pattern of growth even when corrected for ICV. This means that the amygdala is growing at a faster rate than ICV before 12 weeks of age, and then slowing down from 12 to 24 weeks of age. This growth pattern has been linked to the functional role of the amygdala in humans and macaques. Human infants begin to experience separation anxiety at 7-10 months of age, which has been linked with the threat activation and increased volume and functional connectivity of the amygdala (Herschkowitz 2000). A similar anxiety activation has been reported in infant rhesus macaques of equivalent age (~8weeks) during human intruder tasks (Coleman and Pierre 2014). This fast amygdala growth and the activation of threat-detection system early is important for humans and monkeys. In monkeys, weaning around 12 weeks of age (Reitsema et al. 2016; Suomi 2005a) during which they are beginning to explore more on their own and spend more time with peers, and for humans, 7-10 months is the time when an important developmental milestone -crawling- begins (Adolph et al. 2011) and infants start exploring their surroundings. Similar developmental patterns have been reported in rodents, with a functional amygdala emerging at 10 days after birth (corresponding to 9-10 months in human infants) and threat-learning appearing for the first time at this age (Graham et al. 2016; Sullivan 2017). Thus, the developmental trajectory of amygdala growth

seems perfectly timed to each species biological needs. During early development and the period of rapid amygdala growth, infants (rodents, macaques, and humans) are forming attachment bonds with their caregivers (Sullivan 2017). The relationship with the primary caregiver during this time period significantly alters amygdala structure and function (Sullivan 2017). In humans, mother's presence attenuates amygdala activity through a reduction in the amount of stress hormones in the infant. Infants with early life adversity have larger amygdala's than those that did not face these early challenges (Roth and Sullivan 2005; Sanchez 2006; Sullivan 2017; Sullivan and Toubas 1998). In summary, the results of this study, in conjunction with previous work suggests that weaning and increased locomotion, independence and exploration (7-10 months in humans; around 12 weeks in macaques) could be a critical period in development that should be further investigated for intervention in a variety of disorders, including ASD where individuals with ASD show differences in fear experiences and in the identification of trustworthy facial features than typically developing individuals (Baron-Cohen et al. 2000; Ewing et al. 2015a).

Most of the ROIs showed a slowing in growth after 12 weeks of age (except for the TPO, which grew continuously). It is known that overall brain growth slows down after the initial phase of drastic growth during infancy, as the brain regions become closer to their adulthood size, and the rate of synaptogenesis begins to slow and pruning starts (Liu et al. 2015; Malkova et al. 2006; Scott et al. 2016). Interestingly, there is a major developmental milestone associated with this time point. In macaques, at 12 weeks of age the weaning period has started, where infants begin to spend less time with their mother and more time playing with peers (Reitsema et al. 2016; Suomi 2005a). This period is associated with learning how to process social situations more efficiently. For example, the way both human and macaque infants process faces changes

significantly during this time, with decreased in the amount of face looking time occurring during the weaning period and an increase afterwards (Muschinski et al. 2016). It is possible that the reduction in social brain regions growth rate is connected with a social experience. In humans, this time point (1 year of age) corresponds to many important events, but specifically, this is first time point where differences in head size, and thus brain volume, are linked to a diagnosis of ASD later in life (Hazlett et al. 2017). Larger head circumferences measured at 9-14 months are correlated with a 59% higher chance of being diagnosed with ASD (Courchesne et al. 2003). Though the specific functional consequence of this increased brain size is unknown, it suggests one of two things. First, there may be a biological checkpoint for typically developing individuals at this age that is being surpassed/ overridden by individuals with ASD. Second, because the social experience of children with ASD is remarkably different from typically developing children (Ewing et al. 2015b; Schultz et al. 2000; Wing and Gould 1979), based on how they receive, process, and produce social behaviors, the brain isn't getting the same input to allow regions to refine their processing steps without increasing in volume. Due to the developmental importance of this time period, future studies should investigate the implications of the growth plateau to determine if it is a critical period in development and if intervention at this time period is beneficial for children with ASD.

The results from the eye-tracking data are also consistent with previous research. Previous eye-tracking studies have shown that both monkeys and humans spend more time looking at faces, than at the background of stimuli surrounding faces (Frank et al. 2009; Johnson et al. 1991; Nahm et al. 1997). While human studies have shown that preference for faces arises as early as one hour after birth, our data suggests this phenomenon didn't happen until 3 weeks of age in macaques. This discrepancy could be due to small sample size for eye-tracking data

collected before 3 weeks of age. There were only 2 subjects that viewed the stimuli at 1 week of age and 6 subjects at 2 weeks of age, after this time point there was data from 8-14 subjects at each time point. Despite this difference, the fact that our study maintained the preference for faces over background stimuli at a young age is important because it suggests that the subjects in our study process faces as expected developmentally. Whether or not macaques can detect or understand trustworthiness is a controversial topic (de Waal 2014), therefore it is vital that our results are consistent with previous face processing data because it shows that our stimuli were recognized and processed as faces by the macaques. Altruism and deception are very common in the great apes, however the existence of purposeful deceit and loyalty is not known in monkeys (de Waal 2014). Despite uncertainty, there are acts that show signs of trustworthiness and untrustworthiness, for example acts of sneaky mating shows intentional deceit, and monkeys have shown to reject unequal pay, indicates an understanding of fairness and expectation of trust (Brosnan and De Waal 2003; de Waal 2014). Future studies are needed to determine whether or not macaques can conceptualize trust and intentionally display trustworthiness and untrustworthiness.

Furthermore, the longitudinal trajectory for the average time spent viewing faces in this study replicates finding from previous studies. A prior study showed an increase in time spent viewing faces with direct eye-gaze from 0-5weeks of age, a decrease in time from 5-18 weeks of age, and then an increase in time from 18-24 weeks of age (Muschinski et al. 2016). This has a striking parallel with the developmental pattern showed by our subjects when viewing the human faces (especially the trustworthy faces). In NHPs, faces with direct eye-gaze signify two things, a threat, or an opportunity to engage in mutual communication. Muschinski and colleagues (2016) explain the peak in fixation on face with direct eye gaze by describing a critical period in

development between 4-9 weeks in monkeys (and 4-5 months of age in humans) during which there is an emergence of gaze related abilities (Grossmann et al. 2008; Grossmann et al. 2013; Muschinski et al. 2016). Previous experiments have shown that mutual gaze skills at this time period are related to the reactivity of temporal and prefrontal cortices in humans and that gaze behavior stabilizes shortly after, between 6 and 8 months of age (Grossmann et al. 2008; Grossmann et al. 2013; Muschinski et al. 2016). In humans, early emergence of gaze skills has been related to the age of predicted language acquisition and theory of mind skills in toddlers. In monkeys, these ages are associated with gaining social skills during the weaning period. These studies in conjunction with our results suggest that human trustworthy faces portray an opportunity for joint communication and attention. In contrast with the findings for human faces, the results for the developmental trajectory of time spent looking at the monkey faces were "flat", showing no significant changes with age. There is a chance that there is a difference in valence between the human and monkey faces that caused this result, or this result could be explained by the large amount of missing data, or the excessive variability in looking time between subjects effecting the average curve at certain points.

Another interesting finding was the increase in looking time at the monkey mouths with age, in relation to both total time of stimuli exposure and time looking at faces. This is not a surprising result because macaques get a large amount of social information from the mouth, with yawning and open mouths signifying threats, grinning and bared-teeth being a sign of fear or submission, and lip-smacking being a pro-social sign (Parr and Heintz 2009; Sterck and Goossens 2008). Thus, as infant monkeys get older and spend more time with peers, they begin to learn these social cues, and would begin to learn to pay attention to them. This trend of increased time looking at the mouth with age has also seen in a human infant study. It was found

that looking time at the mouth of faces increased with from birth to age two for both typically developing children and children with ASD (Jones et al. 2015). While this result in humans has been associated with language development (Lewkowicz and Hansen-Tift 2012), it shows that there may be similar social developmental processes underlying visual-social engagement across humans and macaques. The macaques only showed this increase in mouth looking time with age when viewing the monkey stimuli, suggesting that this is a species-specific effect. Previous research has shown that in human infants species-specific perceptual narrowing occurs as early as 9 months of age (Pascalis et al. 2002). Human infants can discriminate between different monkey faces as well as they can different human faces at 6 months of age, but by 9-months they are significantly better at discriminating between human faces than they are at monkey faces (Pascalis et al. 2002). In order to determine if this is a species-specific phenomenon, future studies should investigate whether this trend in mouth looking time is seen in human infants while viewing non-human primate faces.

Lastly, there was no significant preference for looking at the trustworthy or untrustworthy faces, even at 24 weeks of age. This result was contradictory to my hypothesis. Previous studies have illustrated that macaques show a preference for viewing faces with a direct gaze (threatening) over an averted gaze (non-threatening) from 0-4 months of age, and then again at 6 months of age, with the curve looking similar to that of this study's trustworthy human face data (Muschinski et al. 2016). This difference in results could be explained by the difference in skill level needed to detect threat from a direct gaze than from an untrustworthy face. In humans, preference for viewing a face with a direct gaze emerges shortly after birth, but the ability to judge the trustworthiness of faces does not solidify until 5 years of age, and performance at adult level doesn't occur until age 10 (Ewing et al. 2015b). This implies that judging trustworthiness is

a more complex skill than detecting a general threat, and thus it is possible that macaques would show a preference for either the untrustworthy or trustworthy face later in life.

When comparing the structural MRI and eye-tracking data, there is an interesting observation: the time period of slower ROI growth (around 12 weeks of age) overlaps with the time period of decline in looking time at faces (5-18 weeks of age). Previous literature has examined the reason for this decline in face looking time, and it is thought that during this time period both human and macaque infants are learning a more efficient way of scanning faces (Klin and Jones 2008; Parr and Heintz 2009). It is possible that the brain is also transitioning to a more efficient processing mode at this time, with functional connectivity and myelination increasing significantly at this age (Chevalier et al. 2015; Kovacs-Balint et al. 2018). More research would be needed to investigate what is changing in the brain at a cellular/molecular level during this time period as well as the potential correlational and causal relationship between the brain growth and eye-tracking results.

There are several limitations in this study. First, there is no prior research demonstrating macaques' ability to judge or display trustworthiness; thus, there is no evidence to support that the macaque face stimuli that were denoted as trustworthy and untrustworthy in this experiment actually reflect such a construct and has ethological validity in the macaque social environment. To verify these facial characteristics, future studies would be needed to investigate the facial expressions macaques exhibit while they are being deceitful and when they are cooperating. Now, given this caveat, the results presented in this study still show macaques' ability to distinguish between subtle facial expression differences in the same face. Because children with ASD also struggle with this skill (Rump et al. 2009), the findings from this study are relevant. A second limitation was the high amount of missing eye-tracking data per animal, which

challenged the statistical analysis. Analyzing a few subjects at a few time points does not accurately represent the data as a whole. Future studies should use a multilevel modeling statistical approach to evaluate the eye-tracking data to address the problem of the missing data. Lastly, future studies should examine the associations between developmental trajectories of structural MRI and eye-tracking data to examine relationships between brain growth and the visual processing of faces.

Despite these limitations, this study is unique and serves an important role in our knowledge of brain development. It is one of very few studies investigating the development of the infant rhesus macaque brain in such detail early in development, most studies only acquired one or two structural MRI scans during the same developmental time period that this study collected 7 scans. This allows for much more refined examination of growth trajectories and highlights time points for further investigation for possible therapeutic interventions. Furthermore, this is the first study to investigate whether or not macaques can differentiate between trustworthy and untrustworthy faces.

Tables:

Table 1: Average percent looking time at human faces and stimuli background in relation to total time of stimuli presentation.

Age	Face	Background
1	0.465±0.123	0.443±0.0298
2	0.357±0.103	0.505±0.100
3	0.623±0.0840	0.269±0.094
4	0.564±0.074	0.251±0.080
5	0.612±0.095	0.261±0.108
7	0.685±0.054	0.141±0.044
9	0.582±0.096	0.227±0.068
11	0.609±0.082	0.173±0.038
13	0.642±0.078	0.278±0.102
15	0.572±0.065	0.182±0.058
17	0.477±0.15	0.219±0.033
19	0.686±0.023	0.230±0.056
21	0.692±0.044	0.134±0.024
23	0.687±0.047	0.178±0.064

Table 2: Average percent looking time at monkey faces and stimuli background in relation to total time of stimuli presentation.

Age	Face	Background
1	0.556±0.234	0.653±0.025
2	0.471±0.094	0.442±0.132
3	0.600±0.096	0.359±0.085
4	0.558±0.116	0.329±0.116
5	0.713±0.094	0.154±0.073
7	0.708±0.061	0.128±0.022
9	0.526±0.087	0.239±0.063
11	0.661±0.084	0.165±0.035
13	0.722±0.080	0.120±0.037
15	0.675±0.081	0.194±0.010
17	0.637±0.096	0.314±0.123
19	0.823±0.038	0.133±0.040
21	0.834±0.041	0.078±0.023
23	0.665±0.105	0.231±0.105

Table 3: Main Findings

Brain Regions	PFC	Plateau 12-16 weeks of age (absolute volume) Grew at same rate as ICV
	TPO	Grew continuously (absolute volume) Grew at a faster rate than ICV from 12-24 weeks of age
	TE	Plateau 8-16 weeks of age (absolute volume) Grew rapidly (absolute volume and compared to ICV)
	Insula	Plateau 8 weeks of age (absolute volume) Grew at same rate as ICV
	AMY	Grew rapidly from 2-12 weeks of age (absolute volume) Grew rapidly from 2-12 weeks of age (ICV corrected)
Eye-Tracking	Face > Background	Subjects showed a preference for looking at faces compared to background by 3 weeks of age
	Fixation at human face	Unique "U" shaped trend
	Fixation at monkey mouths	Fixation at monkey mouths increased with age

Figures

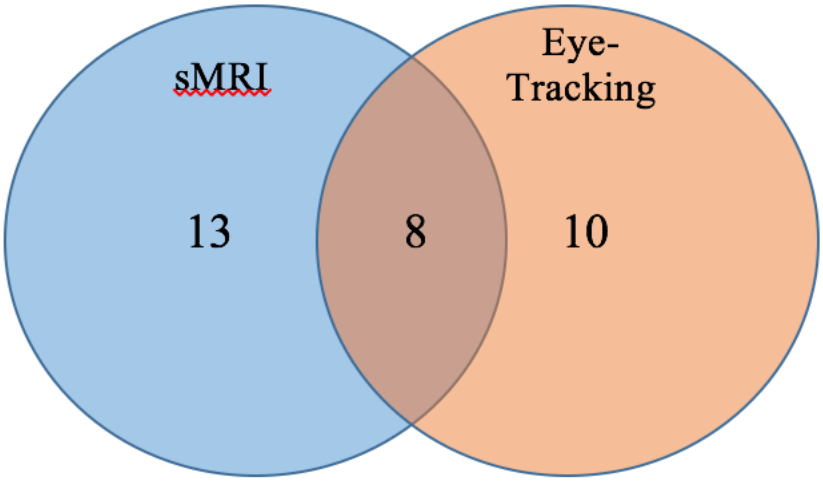

Figure 1: Subjects that participated in each component of the study. 13 subjects participated only in the sMRI study, 10 subjects participated only in the eye-tracking study, and 8 participated in both the sMRI and eye-tracking studies (Total number of subjects: n=31 infant rhesus monkeys).

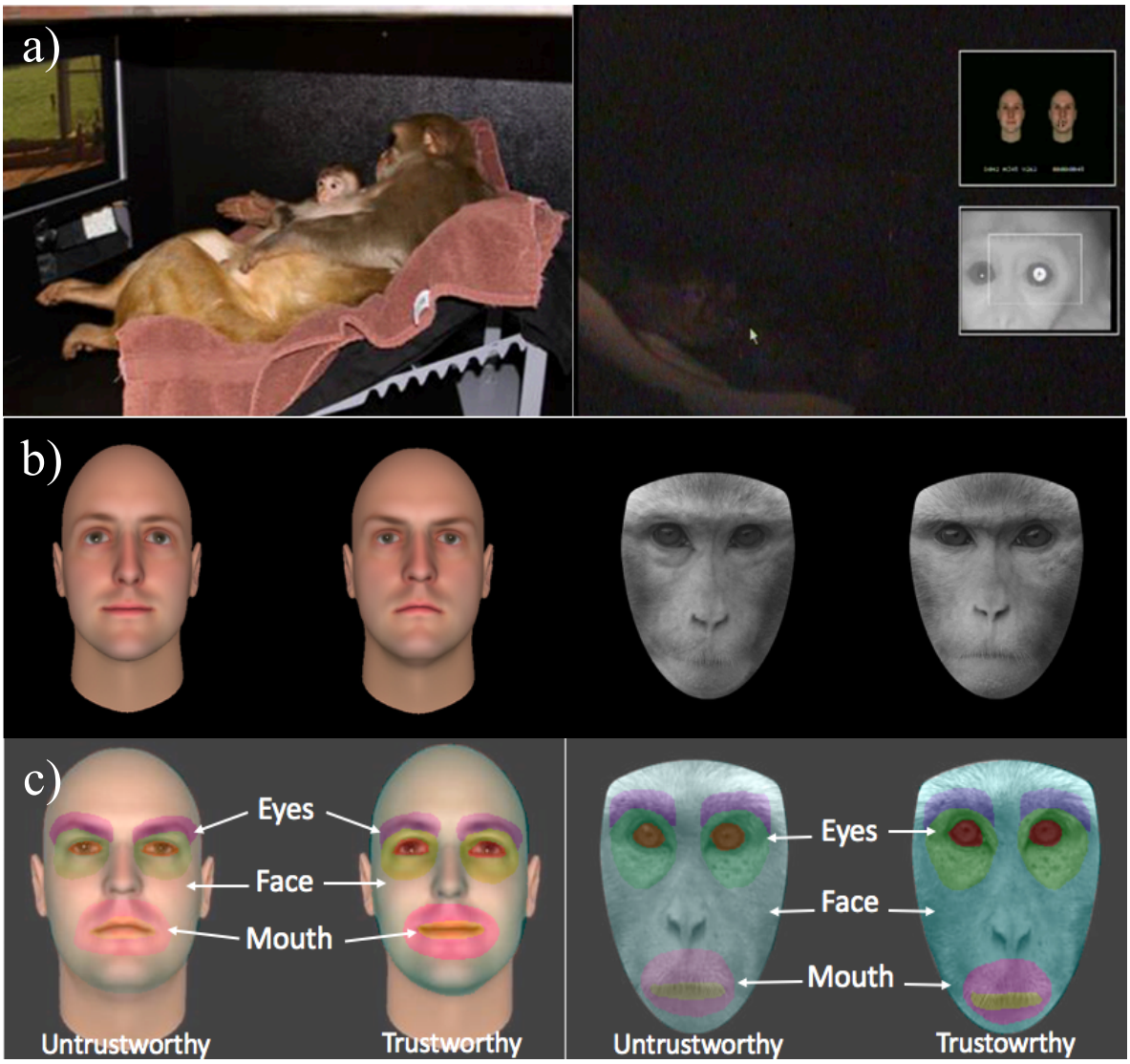

Figure 2: Eye- tracking methods. a) Eye-tracking set up, showing positioning of the infant on the ventrum of the anesthetized mother –left- and calibration of the infant's eyes and stimuli presentation –right. b) Human and monkey stimuli viewed by the subjects. In this example the trustworthy face is on the left and the untrustworthy face is on the right for both species. c) Illustrations of the regions of interest (ROIs) for trustworthy and untrustworthy faces for both species.

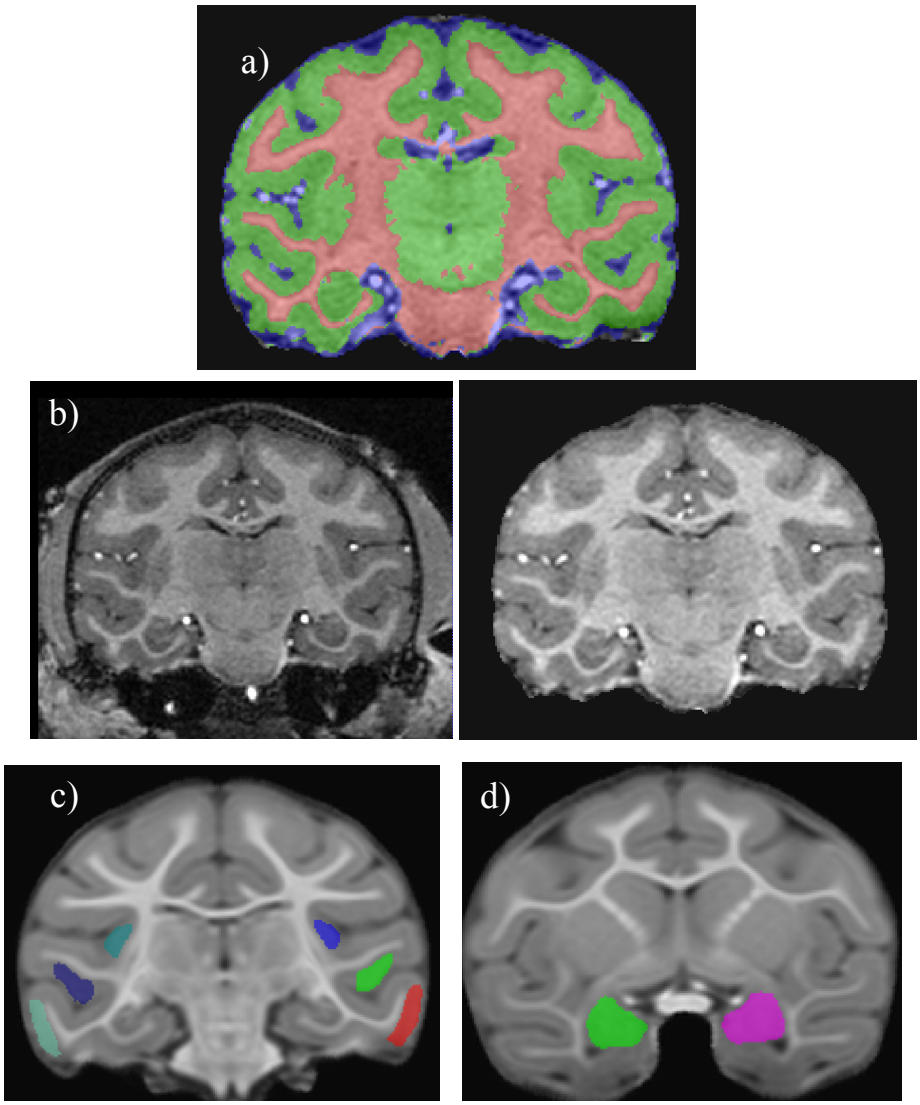

Figure 3: AutoSeg brain registration and segmentation methods. a) Atlas-Based Classification Tissue Segmentation. b) Skull stripping. c, d) Single-atlas subcortical ROI parcellations.

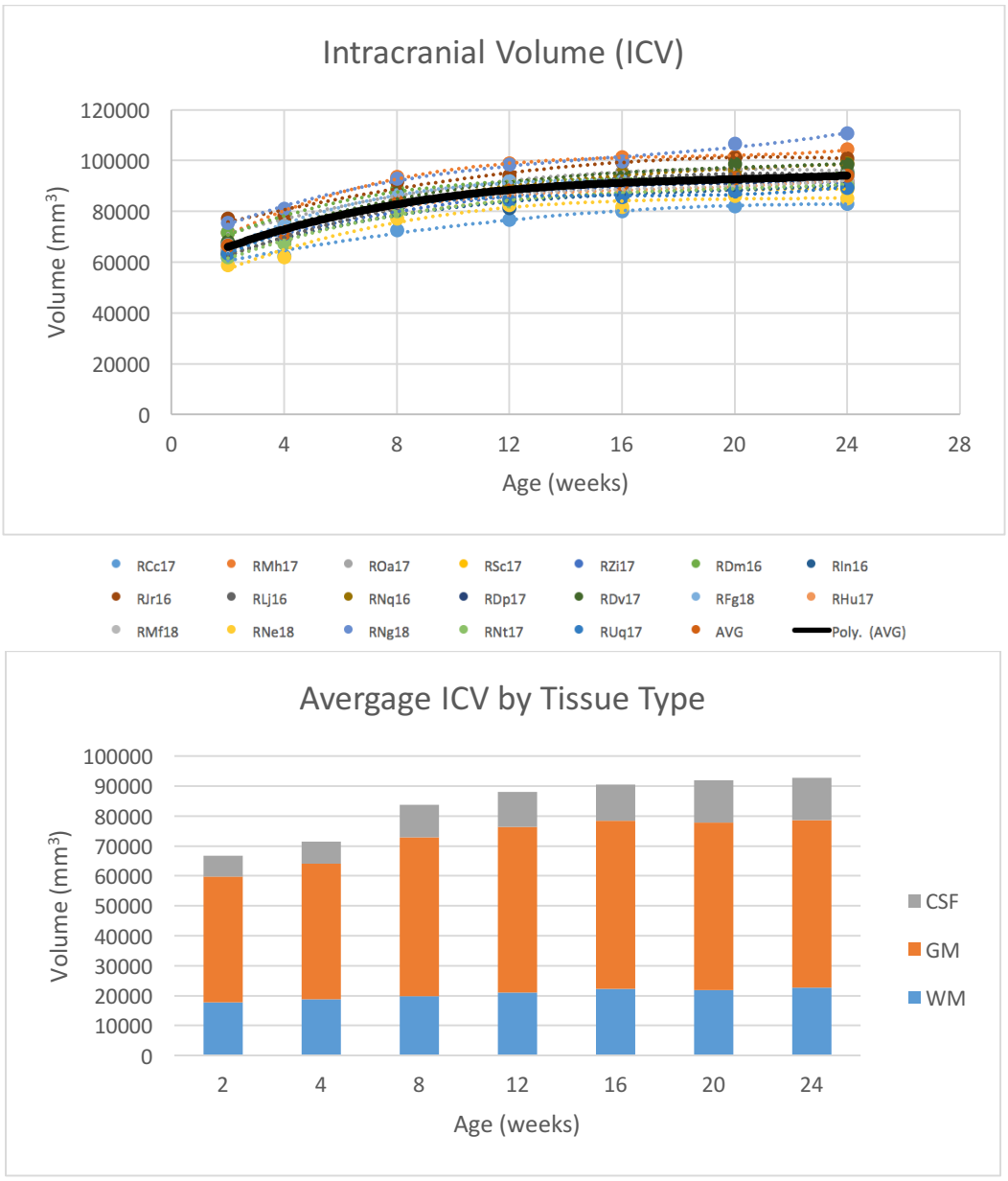

Figure 4: Intracranial volume (ICV) developmental changes by age. a) There was a significant main effect of age ($F(6,108)=667.315$, $p < 0.01$, $\eta 2=0.974$), but no main Hemisphere or Age by Hemisphere interaction effects. Bonferroni pairwise comparisons showed that ICV continuously increased from 2 weeks of age to 23 weeks of age with significant increases in volume between each age points ($p<0.05$). Colored filled circles represent individual subject data and the black line represents the 3rd order polynomial line that best fit the average data points. b) Average ICV developmental changes by age seperated into three tissue classes: GM, WM, CSF.

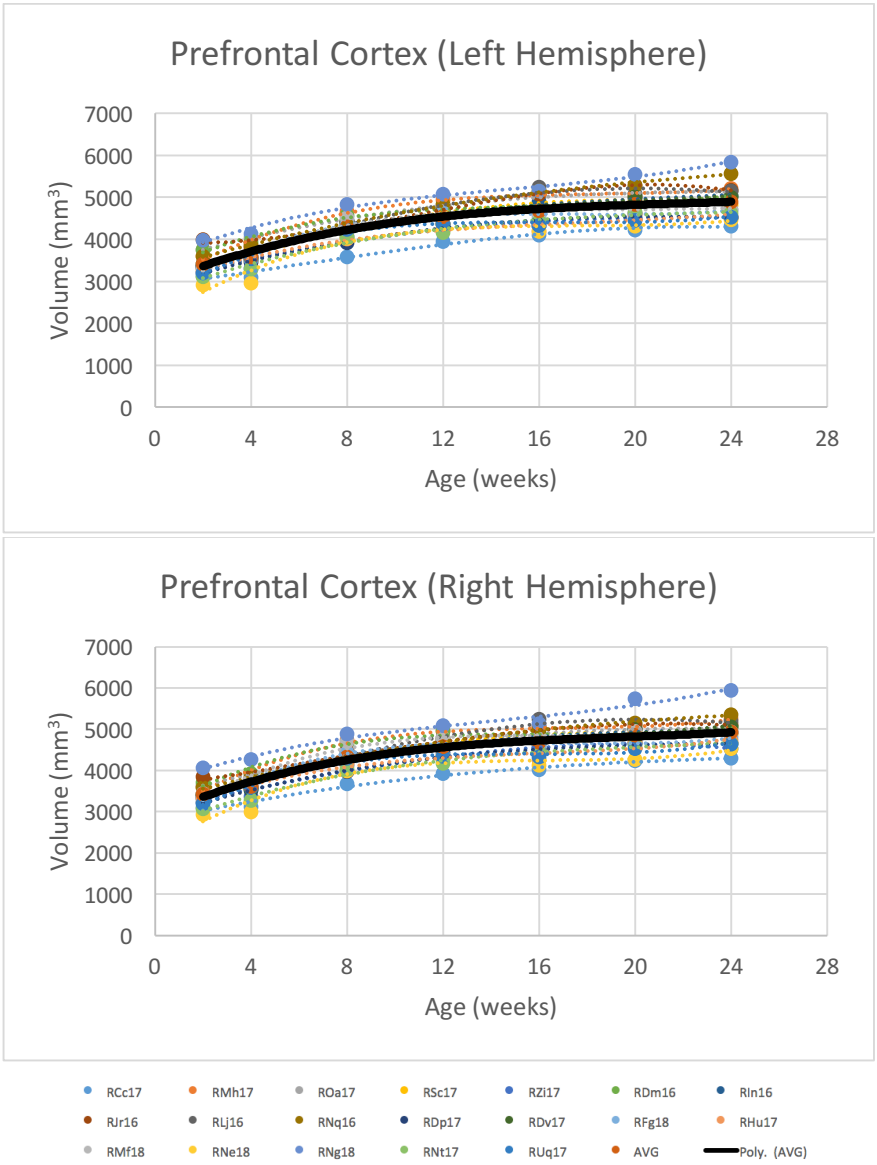

Figure 5: Prefrontal cortex (PFC) volume increased with age. There was a main effect of AGE ($F(6,108)=531.114$, $p < 0.01$, $\eta 2=0.969$; Figure 2). Post-hoc pairwise comparisons showed that the PFC volume grew from 2 weeks of age to 23 weeks of age with significant ($p < 0.01$) increases in volume for most ages, but there was no growth from 12-16 weeks of age ($p=0.260$) and 20-24weeks of age ($p=0.403$). Colored filled circles represent individual subject data and the black line represents the 3rd order polynomial line that best fit the average data points

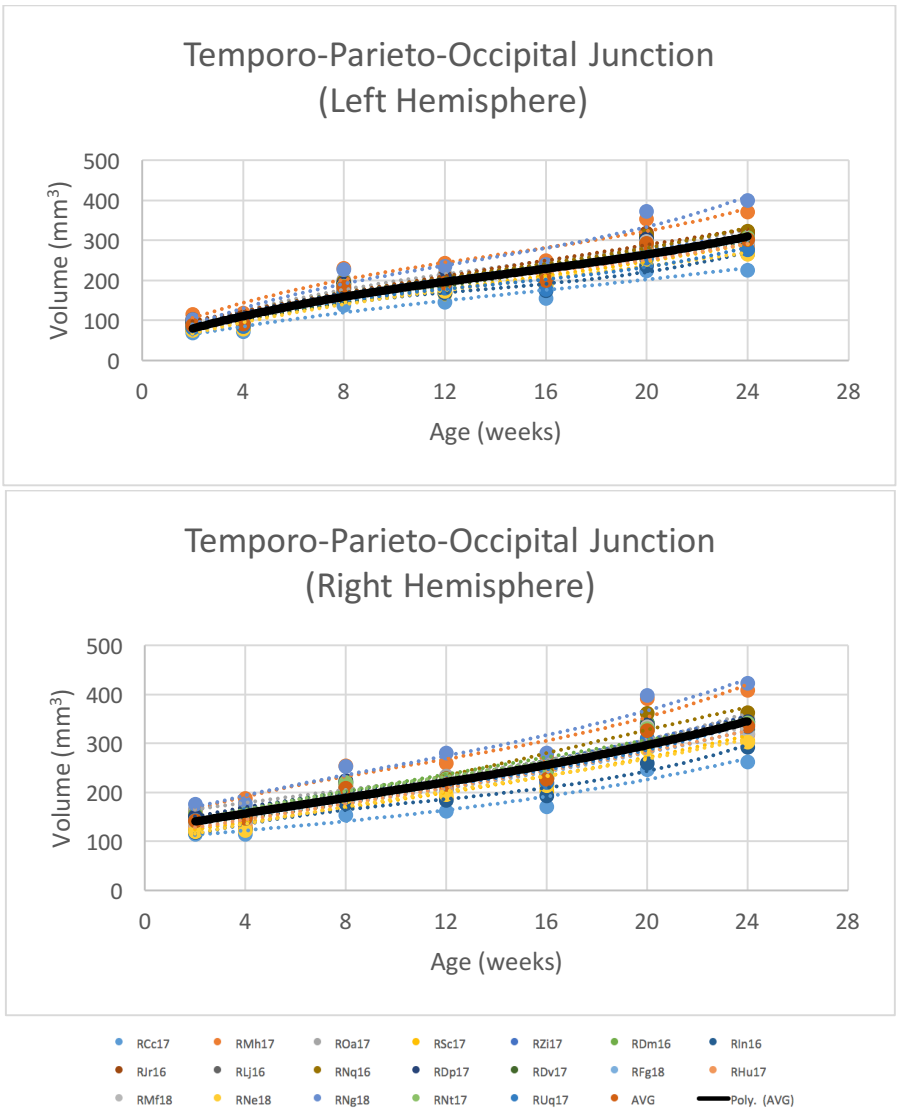

Figure 6: TPO volume increased with age. There are significant main effects of AGE ($F(6,108)=1045.332$, $p < 0.01$, $\eta 2=0.983$), HEMISPHERE ($F(1,18)=419.919$, $p < 0.01$, $\eta 2=0.959$) and an AGE by HEMISPHERE interaction effect ($F(6,108)=87.445$, $p < 0.01$, $\eta 2=0.829$). Post-hoc pairwise comparisons of the means showed that the TPO volume grew continuously from 2 weeks to 23 weeks of age ($p < 0.01$). Colored filled circles represent individual subject data and the black line represents the 3rd order polynomial line that best fit the average data points.

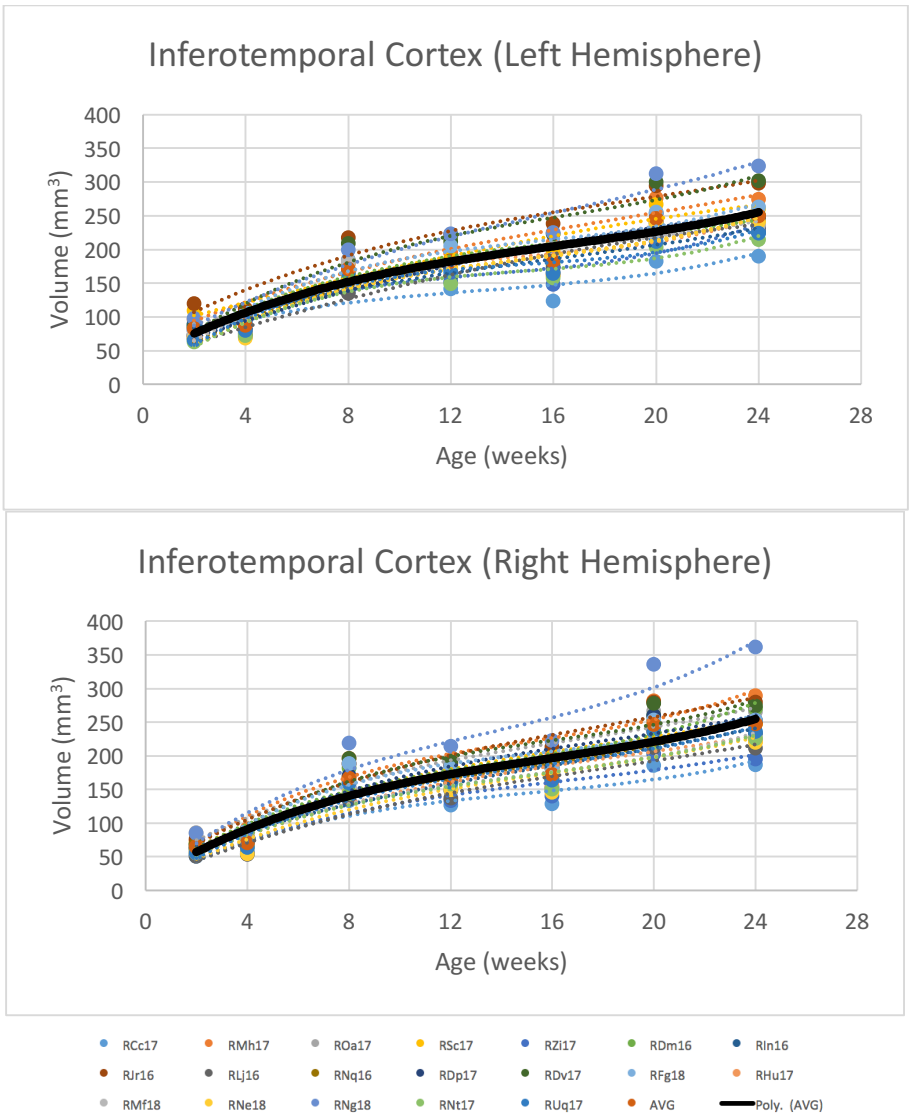

Figure 7: Inferotemporal cortex (TE) volume increased with age. There was a significant main effect of AGE ($F(6,108)=660.691$, $p < 0.01$, $\eta 2=0.973$), HEMISPHERE ($F(1,18)=16.569$, $p=0.001$, $\eta 2=0.479$), and an AGE by HEMISPHERE interaction effect ($F(6,108)=8.573$, $p < 0.01$, $\eta 2=0.323$). Post-hoc pairwise comparisons showed that the TE grew from 2 weeks of age to 23 weeks of age with no growth from 8 weeks to 16 weeks of age (8-12 weeks p=0.11, 8-16weeks p=0.123, 12-16 weeks p=1) and 20-24 weeks of age (p=.306). Colored filled circles represent individual subject data and the black line represents the 3rd order polynomial line that best fit the average data points.

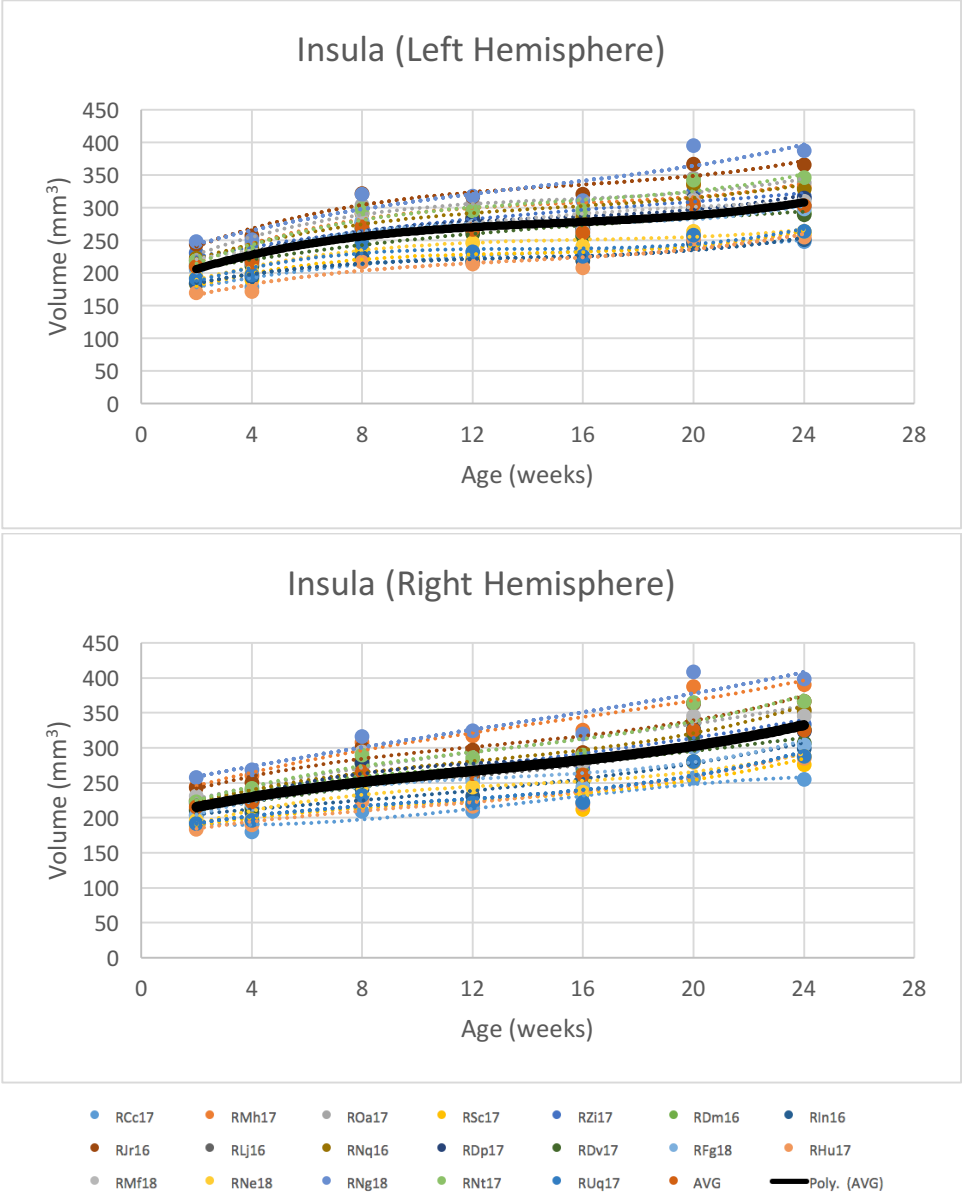

Figure 8: Insula volume increased with age. Main effects of AGE ($F(6,108)=367.224$, $p < 0.01$, $\eta 2=0.953$), HEMISPHERE ($F(1,18)=7.428$ $p = 0.014$, $\eta 2=0.292$) and an AGE by HEMISPHERE interaction effect ($F(6,108)=57.670$ $p < 0.01$, $\eta 2=0.762$) were identified. Post-hoc pairwise comparisons showed that the insula grew from 2-24 weeks of age with a plateau in growth from 8 weeks to 16 weeks of age (8-12 weeks p= 0.82, 12-16 weeks p=0.877) and 20-24 weeks of age (p=1). Colored filled circles represent individual subject data and the black line represents the 3rd order polynomial line that best fit the average data points

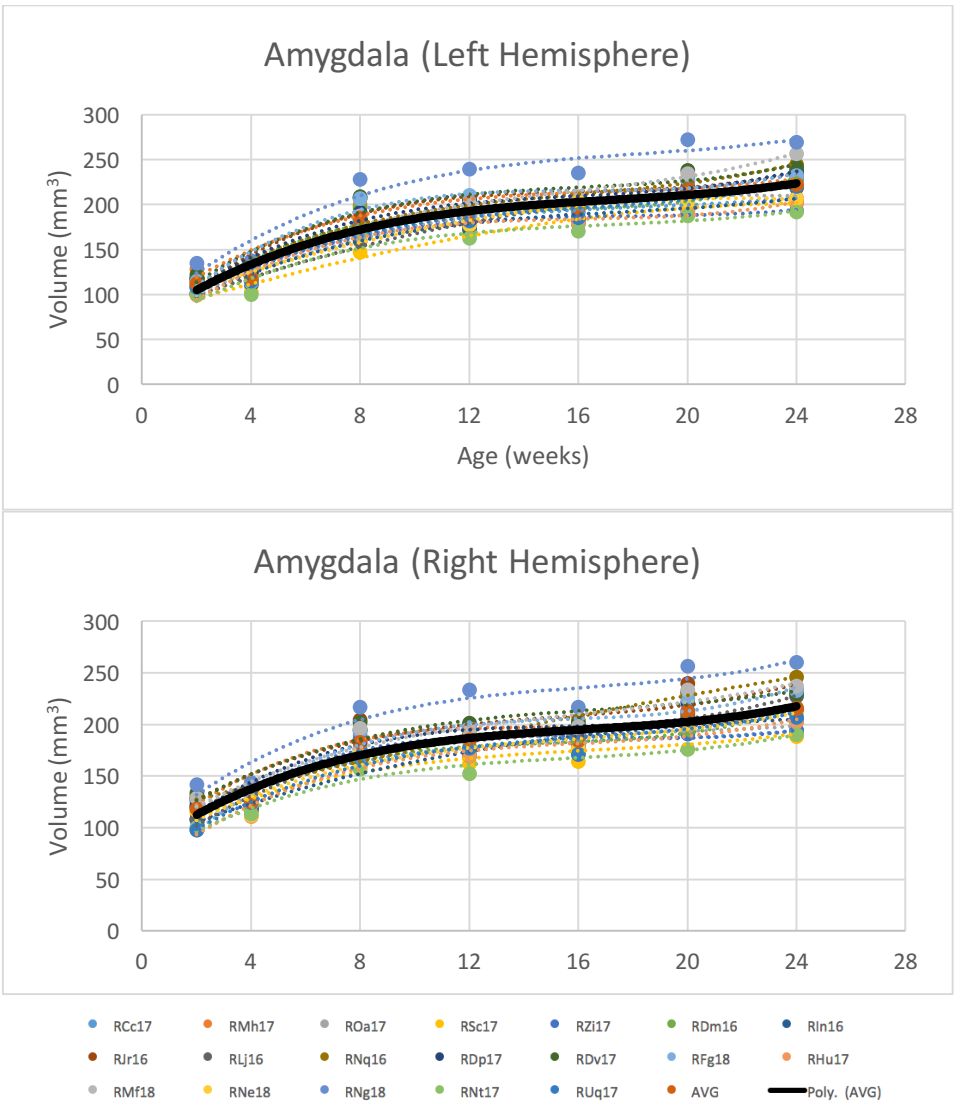

Figure 9: Amygdala volume increased with age. There was a significant AGE effect ($F(6,108)=531.114$, $p < 0.01$, $\eta 2=0.9690$), HEMISPHERE effect ($F(1,18)=5.187$ $p = 0.036$, $\eta 2=0.234$), and AGE*HEMISPHERE interaction ($F(6,108)=11.245$ $p < 0.01$, $\eta 2=.398$). Post-hoc comparisons showed that both the left and right amygdala grew throughout the first 6 months of life, with minimal growth from 8-16 weeks of age (8-12 weeks p=1, 8-16weeks p=0.296, 12-16 weeks p=1), and 20-24 weeks of age and 20-24 weeks of age (p=0.306). Colored filled circles represent individual subject data and the black line represents the 3rd order polynomial line that best fit the average data points

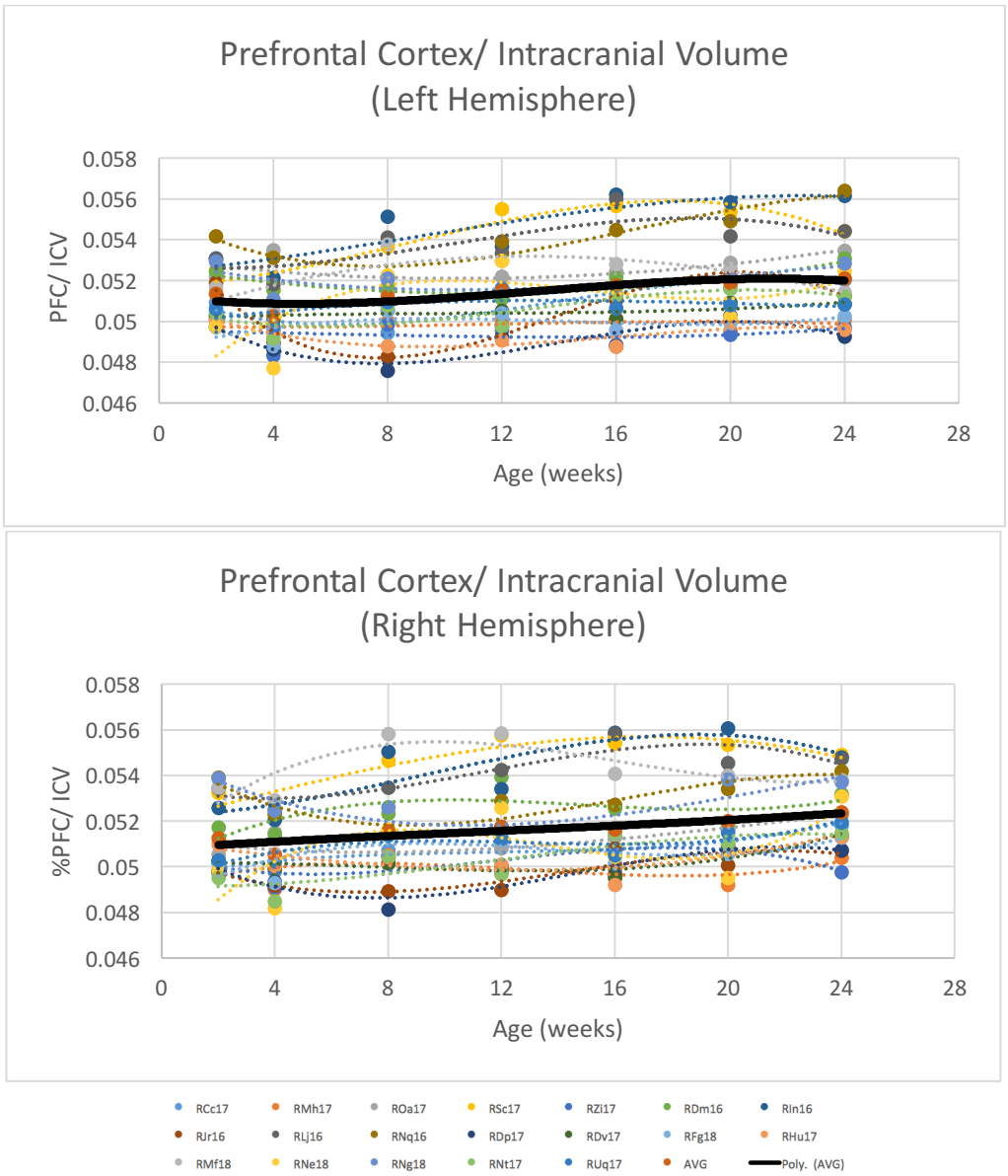

Figure 10: Percent prefrontal cortex volume over intracranial volume change over time. There was a main effect of AGE ($F(6, 108)=10.186$, $p < 0.01$). Post-hoc comparisons showed that there was an increase in volume of the PFC from 2-24 weeks of age ($p<0.01$), however with the exception of significant growth from 2 to 4 weeks of age ($p<0.01$) there was no growth between consecutive ages during the entire time period ($p=1.00$). Colored filled circles represent individual subject data and the black line represents the 3rd order polynomial line that best fit the average data points.

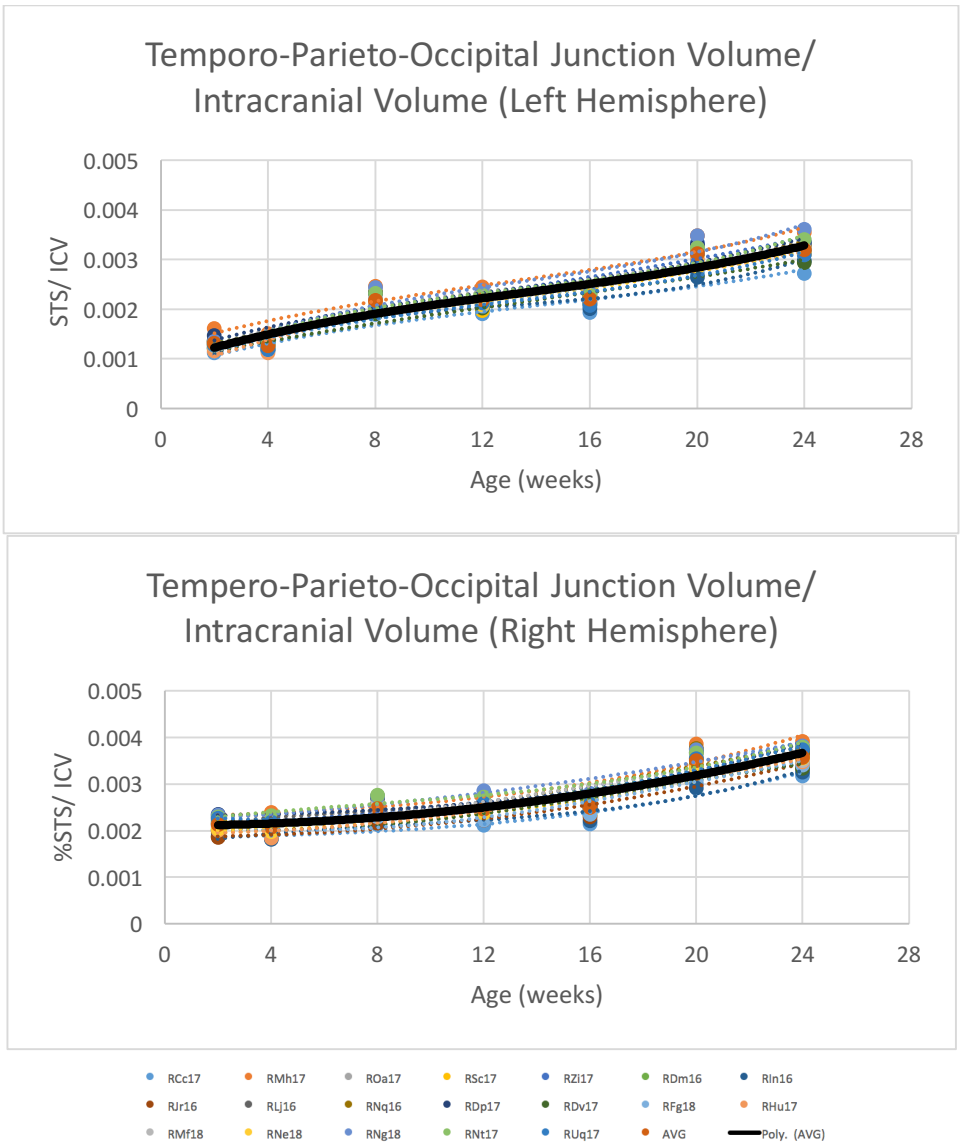

Figure 11: Percent temporo-parieto-occipital junction volume over intracranial volume change over time. Analysis revealed main effects of AGE ($F(6, 108)= 1529.332$, $p < 0.01$), HEMISPHERE ($F(1, 18)=442.082$, $p < 0.01$), and a significant interaction effect of AGE*HEMISPHERE ($F(6, 108)=217.159$, $p < 0.01$). Post-hoc comparisons showed that the TPO grew from 2 to 24 weeks of age ($p<0.05$) with the exception of minimal growth from 8-16 weeks of age and 20-24 weeks of age (8-12 weeks p=1.00, 12-1 6weeks p=1.00, 8-16 weeks p=1.00, and 20-24 weeks p=.109). Colored filled circles represent individual subject data and the black line represents the 3rd order polynomial line that best fit the average data points.

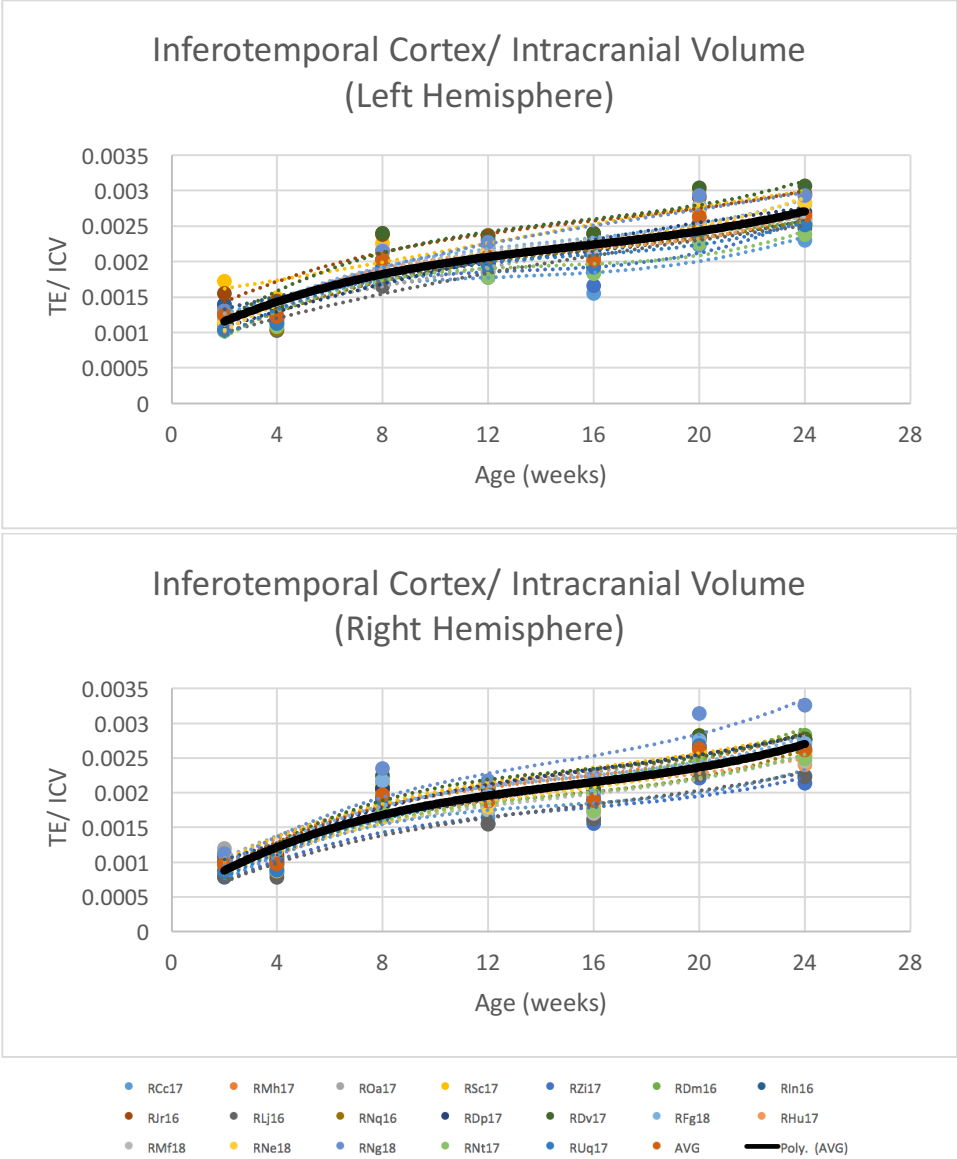

Figure 12: Percent inferotemporal cortex volume over intracranial volume change over time. There were main effects of AGE ($F(6,108)=959.382$, $p < 0.01$), HEMISPHERE ($F(1,18)=20.901$, $p < 0.01$), and an interaction effect of AGE*HEMISPHERE ($F(6,108)=15.824$, $p < 0.001$). Post-hoc comparisons showed that area TE increased in volume over the period of study ($p<0.01$), however, there was minimal growth from 2 to 4 weeks of age ($p=0.996$), and a plateau in growth from 8-16 weeks of age and 20-24 weeks of age (8-12 weeks $p=1.00$, 12-16weeks $p=1.00$, 8-16 weeks $p=1.00$, and 20-24 weeks $p=1.00$). Colored filled circles represent individual subject data and the black line represents the 3rd order polynomial line that best fit the average data points.

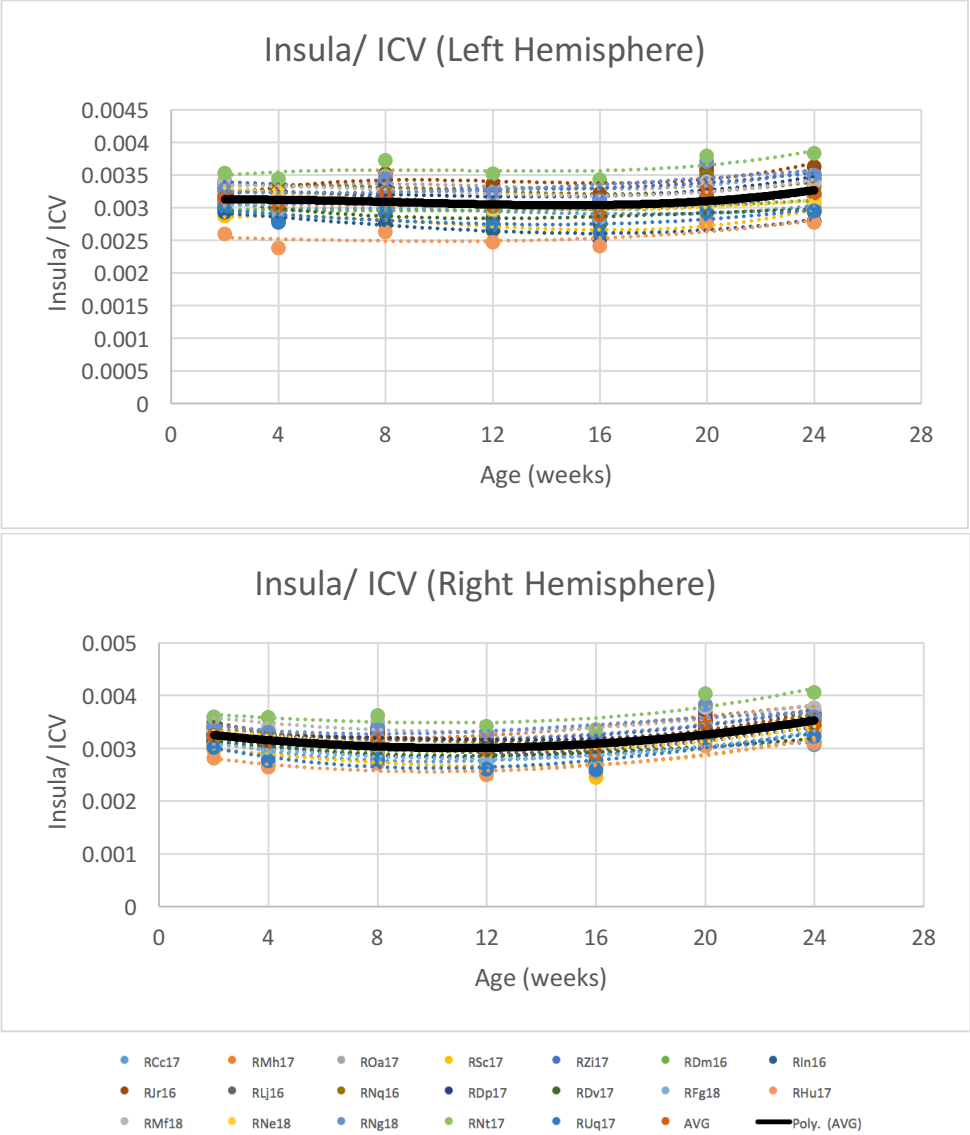

Figure 13: Percent insula volume over intracranial volume change over time. There were main effects of AGE ($F(6, 108)=99.317$, $p < 0.01$), HEMISPHERE ($F(1, 18)= 7.535$, $p = 0.013$), and an interaction effect of AGE*HEMISPHERE ($F(6, 108)=54.005$, $p < 0.01$). Post hoc comparisons showed that there was an increase in volume of the insula from 2 to 24 weeks of age ($p < 0.05$), however there was minimal growth from 20-24 weeks of age ($p=1.00$) and no difference in volume at 2 weeks of age and 8 weeks of age ($p=1.00$). Colored filled circles represent individual subject data and the black line represents the 3rd order polynomial line that best fit the average data points.

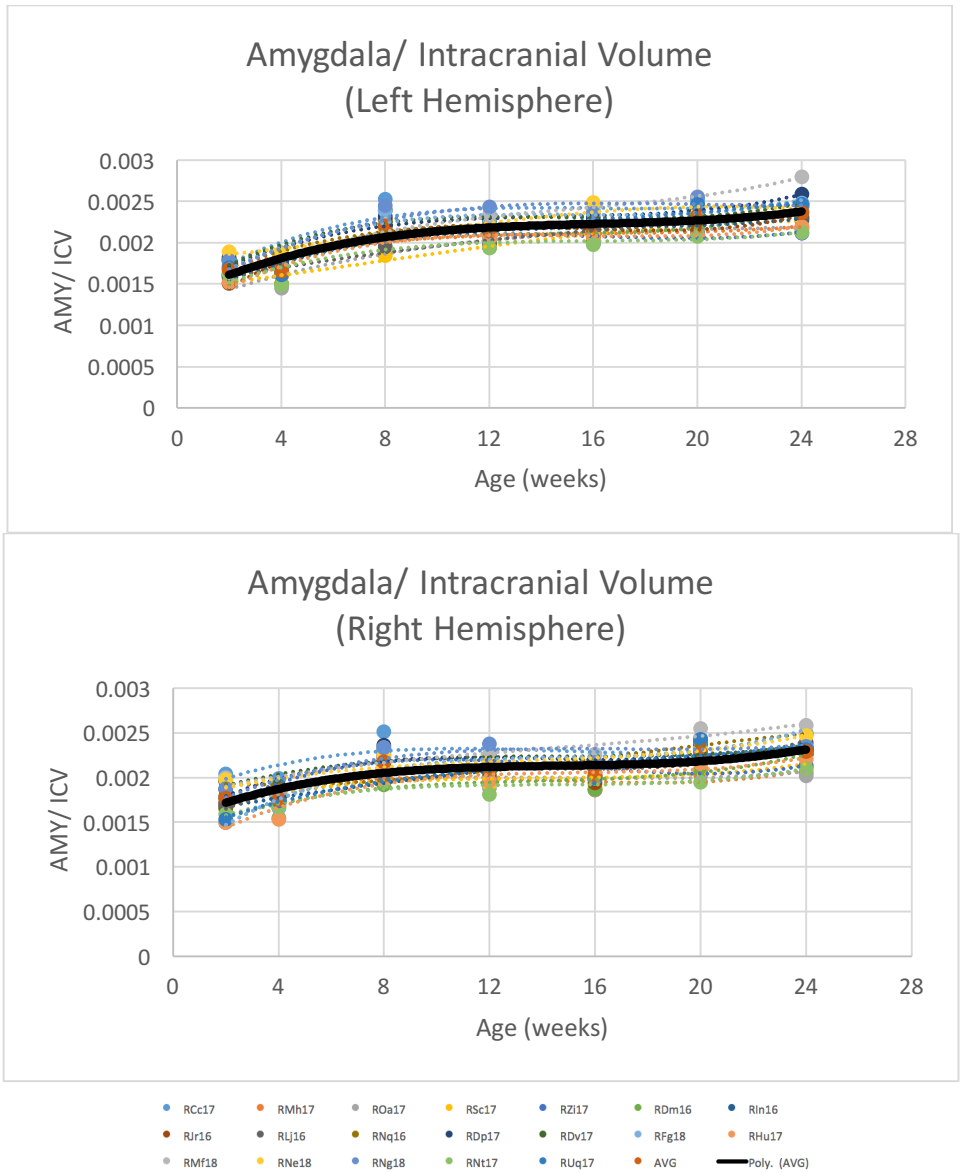

Figure 14: Percent amygdala volume over intracranial volume change over time. Main effects were identified for AGE ($F(6, 108)=201.909$, $p < 0.01$), HEMISPHERE ($F(1, 18)= 3.222$, $p =0.011$), and an interaction effect between AGE*HEMISPHERE ($F(6, 108)=11.981$, $p < 0.01$). There was an increase in AMY volume relative to ICV from 2 to 24 weeks of age, however there was no growth from 2-4 weeks of age ($p=1.00$), 8-16 weeks of age (8-12 weeks $p=0.066$, 12-16 weeks $p=1.00$) and 20-24 weeks of age ($p=1.00$). Colored filled circles represent individual subject data and the black line represents the 3rd order polynomial line that best fit the average data points.

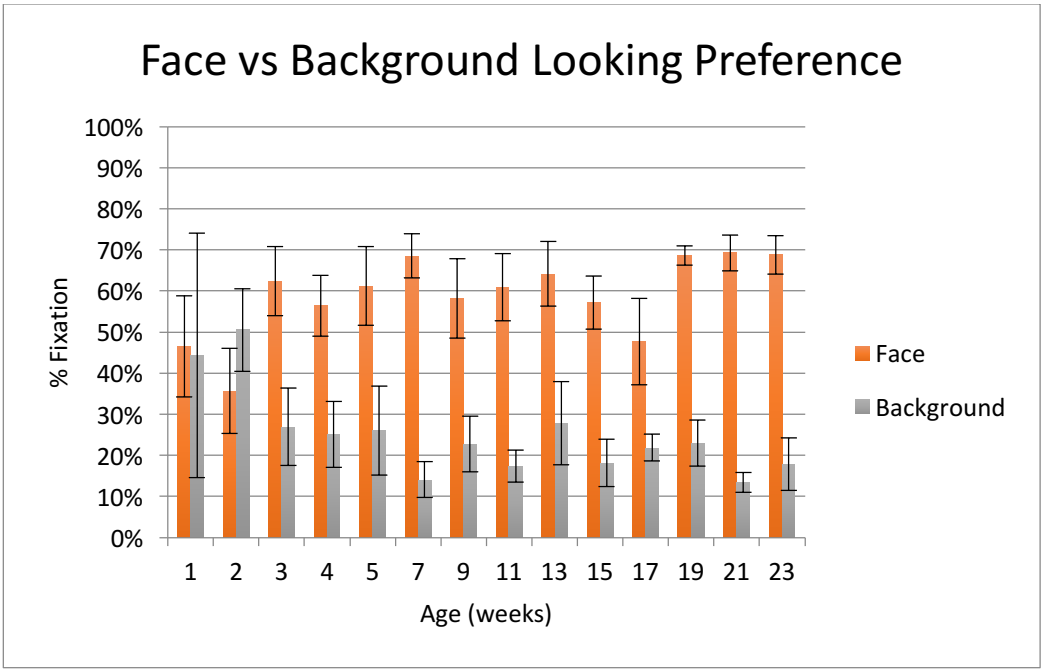

Figure 15: Percent time spent looking at human faces compared to the background of the stimuli. The bars represent the % average time spent looking at faces versus the % time looking at background of the stimuli at each age, and the error bars represent the standard error of the mean (SEM). By 3 weeks of age the subjects prefer human faces to background.

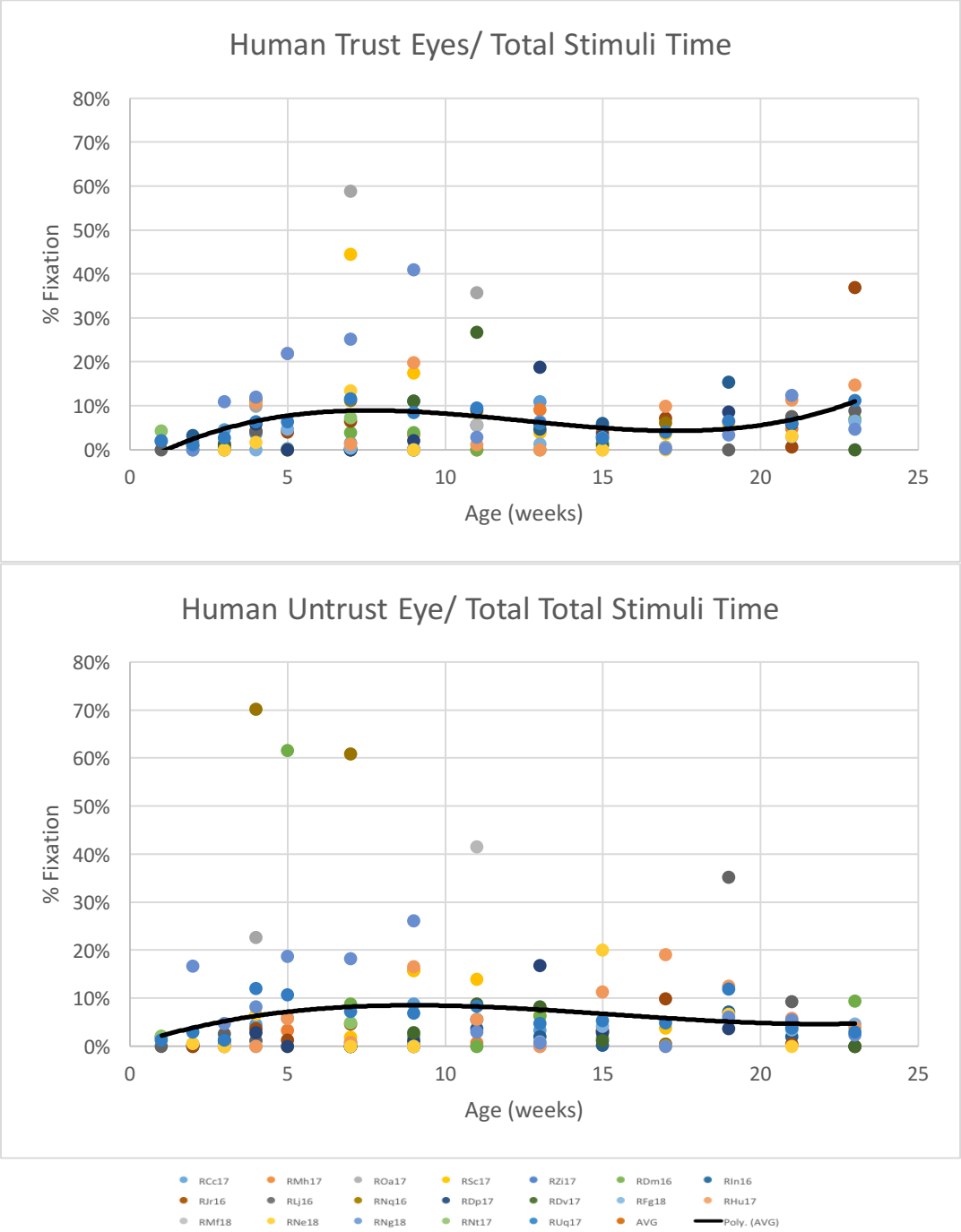

Figure 16: Raw data for percent looking time at human eyes in relation to total stimuli time. Colored filled circles represent individual subject data and the black line represents the 3rd order polynomial line that best fit the average data points.

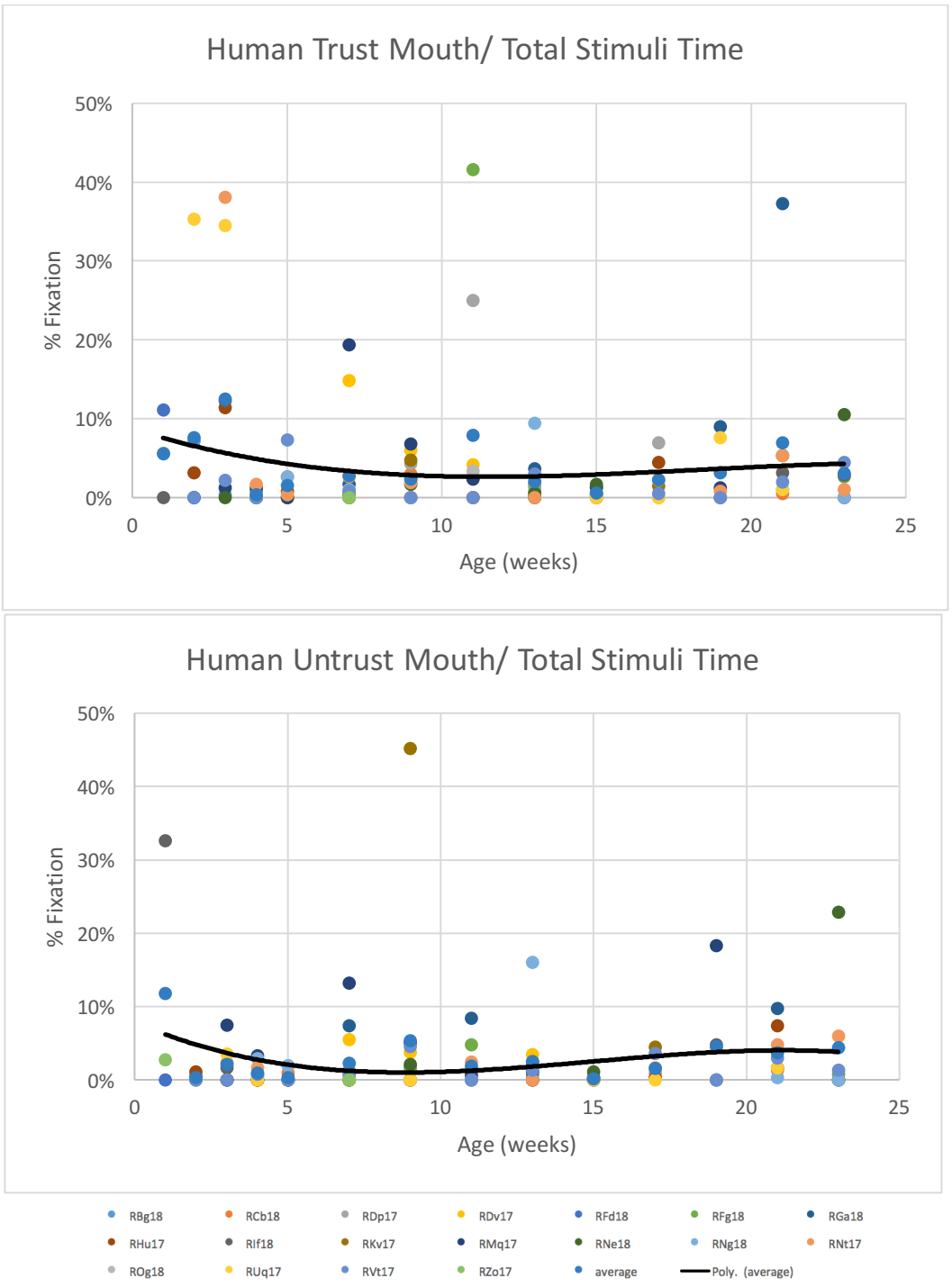

Figure 17: Raw data for percent time looking at human mouths in relation to total stimuli time. Colored filled circles represent individual subject data and the black line represents the 3rd order polynomial line that best fit the average data points.

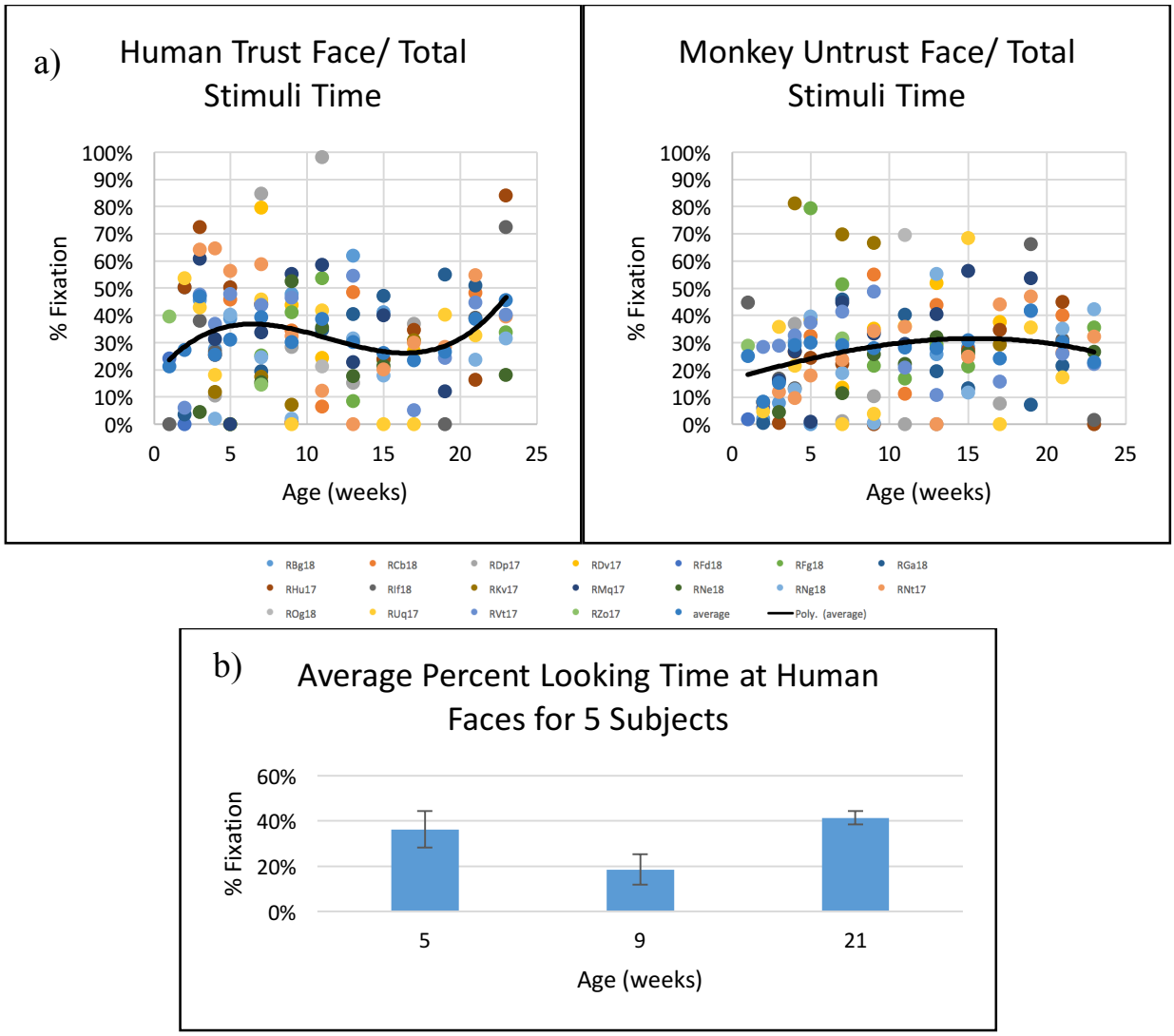

Figure 18: Percent time looking at human faces over total stimuli time. Colored points represent individual subject data and the black line represents the 3rd order polynomial line of best fit for the average data points. a) Raw data for percent looking time at human faces over total stimuli time for all subjects. b) Analysis of 5 subjects at 3 ages revealed a significant main effect of AGE ($F(2, 8)=6.464$, $p=0.021$, $\eta 2=0.618$) that trended towards a decrease in looking time from 5 to 9 weeks of age ($p=0.086$), and then a significant increase in looking time from 9-21 weeks of age ($p=0.009$). The image shows the estimated marginal means for the percentage looking time at faces in relation to total stimuli viewing time and the error bars represent the corrected SEM.

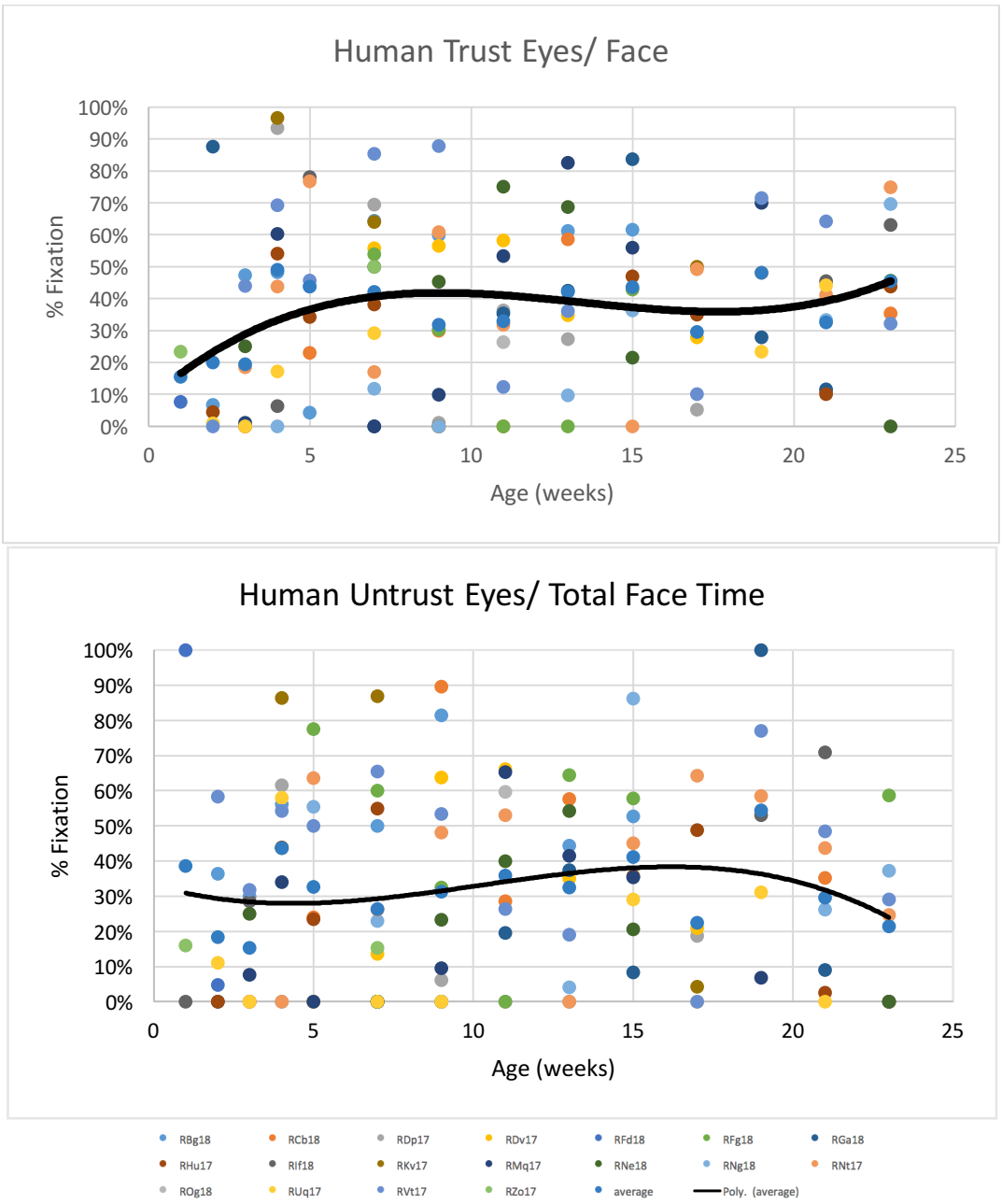

Figure 19: Percent time looking at human eyes in relation to time looking at the whole face. Raw data for percent looking time at human eyes over time looking at the whole face for all subjects. Colored filled circles represent individual subject data and the black line represents the 3rd order polynomial line that best fit the average data points.

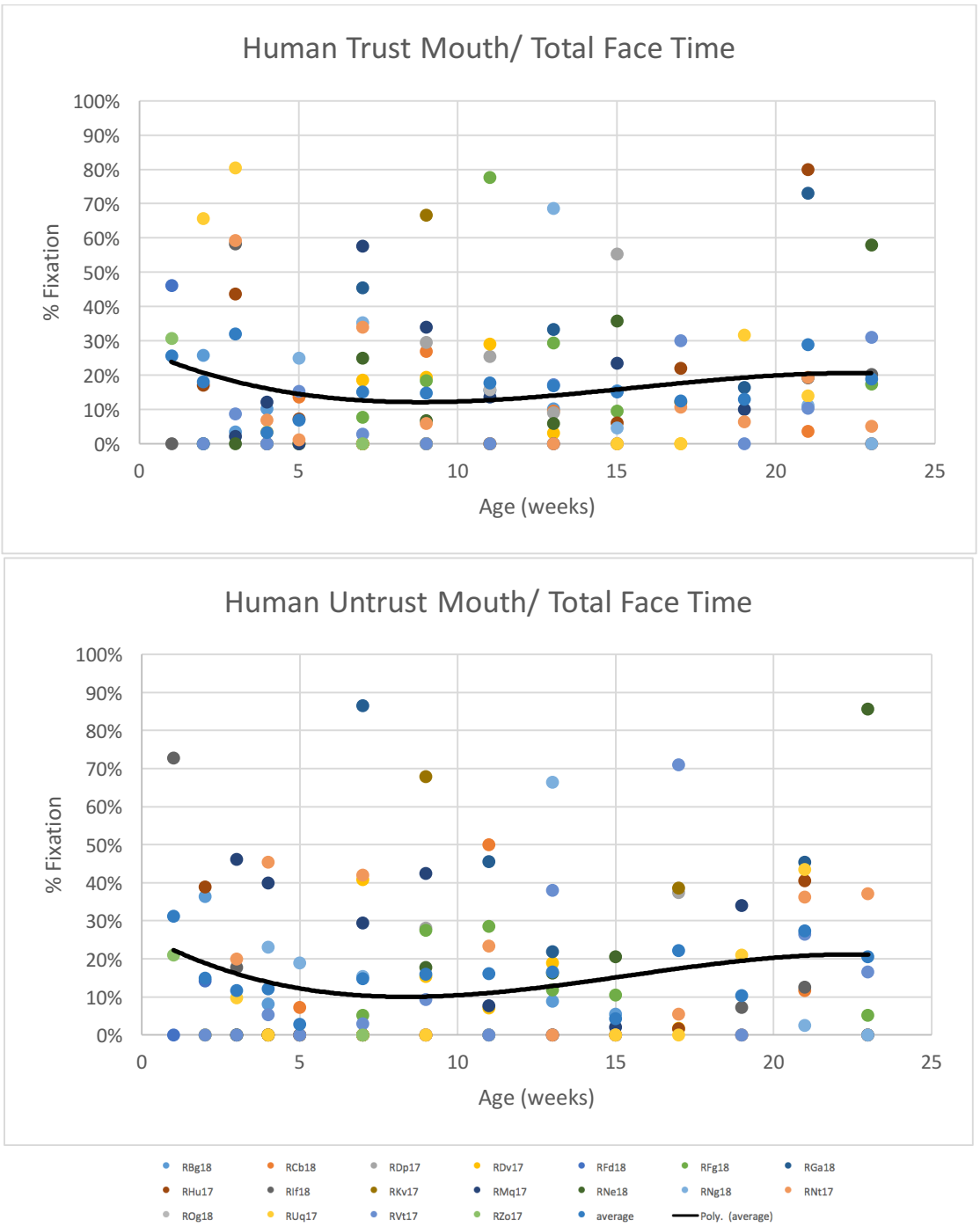

Figure 20: Raw data for percent time looking at human mouths in relation to total time looking at the whole face. Colored filled circles represent individual subject data and the black line represents the 3rd order polynomial line that best fit the average data points.

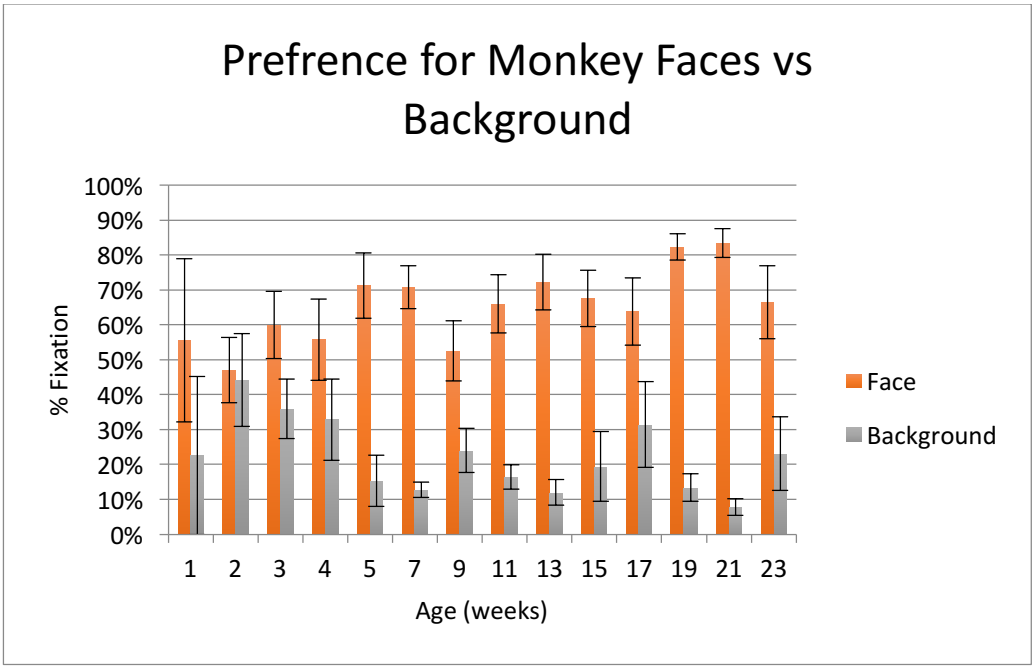

Figure 21: Percent time spent looking at monkey faces compared to the background of the stimuli. The bars represent the % average time spent looking at faces versus the % time looking at background of the stimuli at each age, and the error bars represent the standard error of the mean (SEM). By 3 weeks of age the subjects prefer human faces to background.

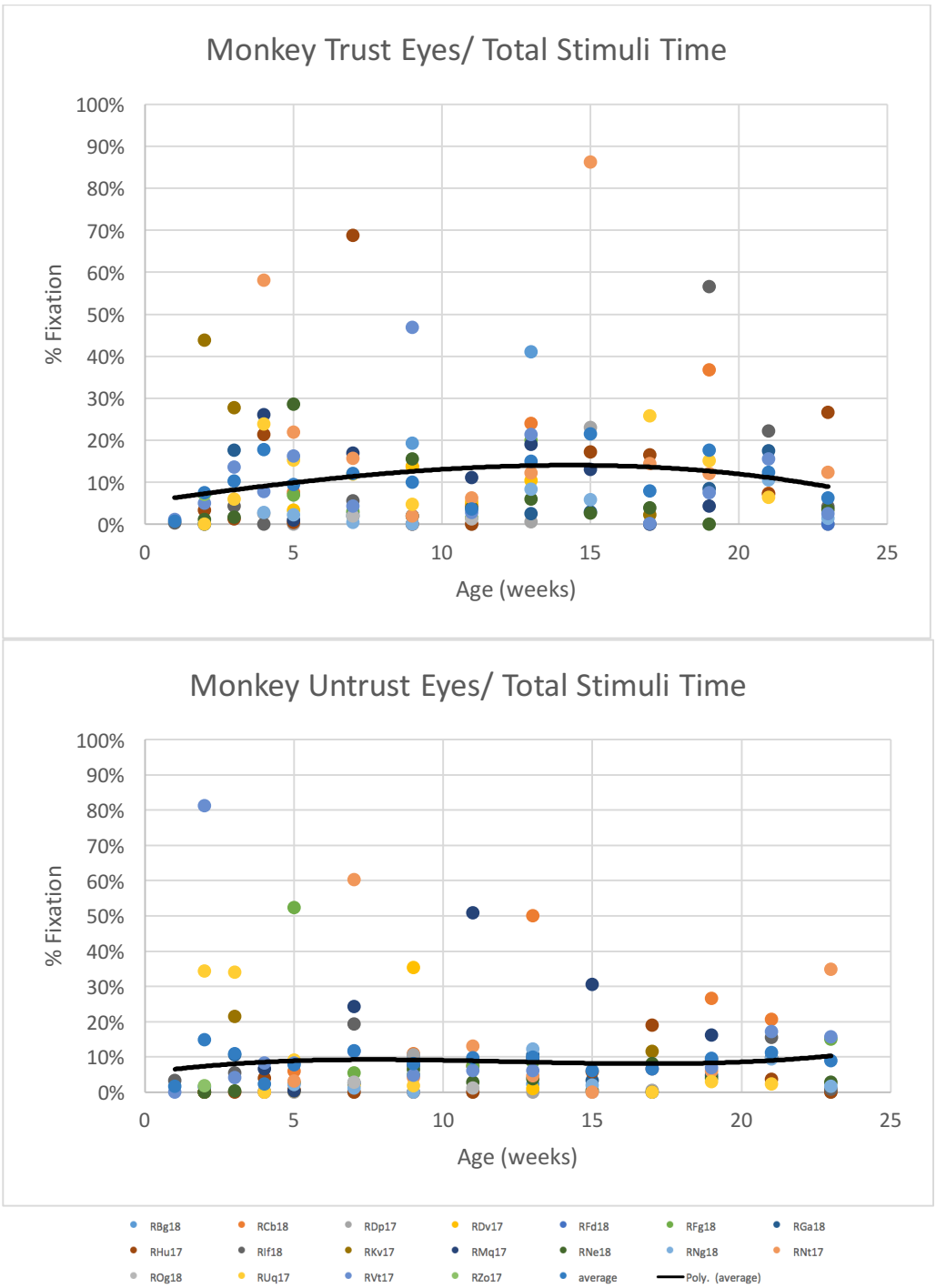

Figure 22: Raw data for percent time looking at monkey eyes in relation to total stimuli time. Colored filled circles represent individual subject data and the black line represents the 3rd order polynomial line that best fit the average data points.

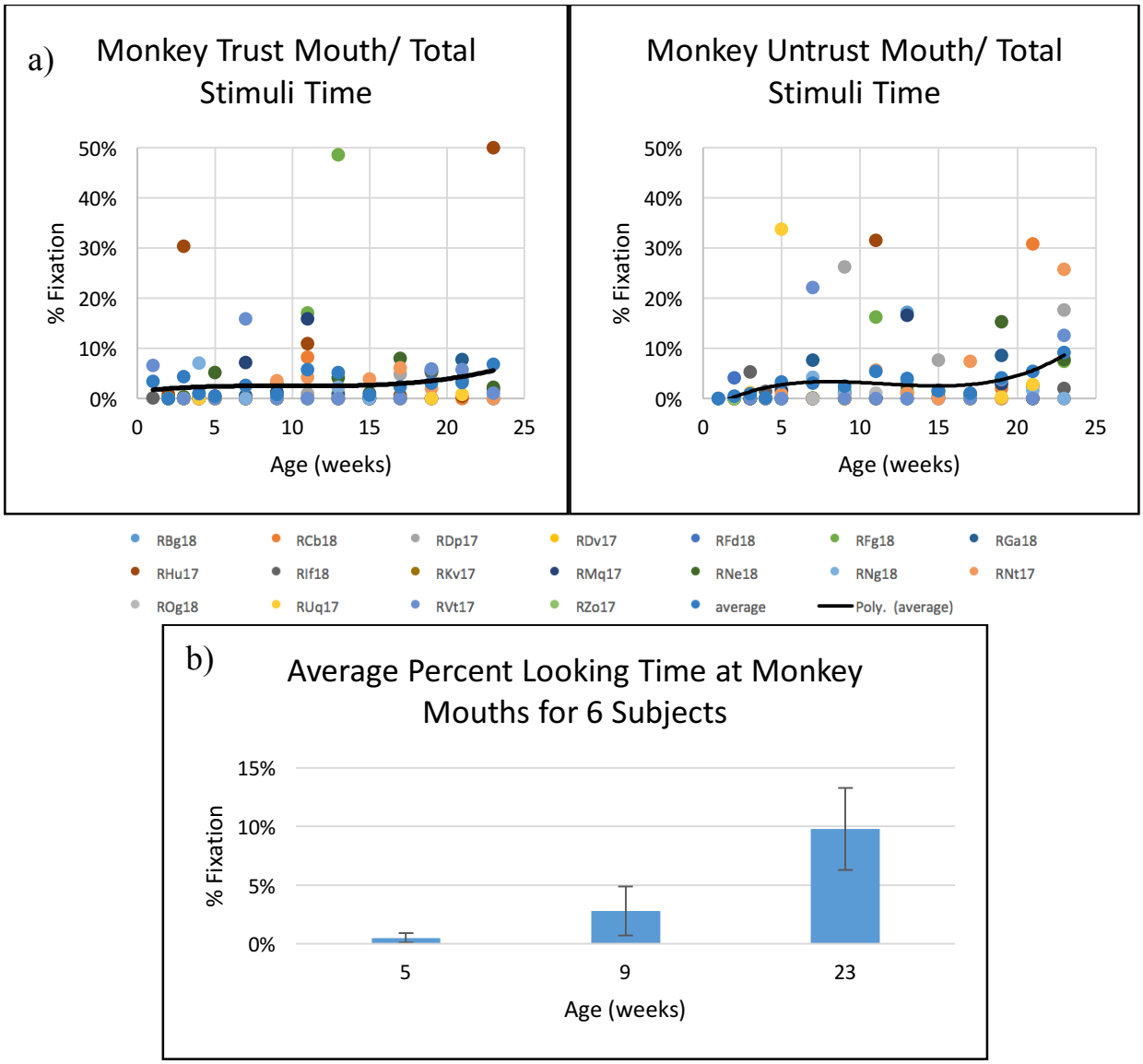

Figure 23: Percent time looking at monkey mouths in relation to total stimuli time. a) Raw data for percent looking time at monkey mouths over total stimuli time for all subjects. Colored points represent individual subject data and the black line represents the 3rd order polynomial line of best fit for the average data points. b) Analysis of 6 subjects at 3 ages revealed a significant main effect of AGE ($F(2, 10)=4.088$, $p =0.05$, $\eta 2=0.450$), with the amount of time spent looking at the mouth of both the trustworthy and untrustworthy face increasing from 5 weeks to 23 weeks of age. The image shows the estimated marginal means for the percentage looking time at mouths in relation to total time and the error bars represent the corrected SEM.

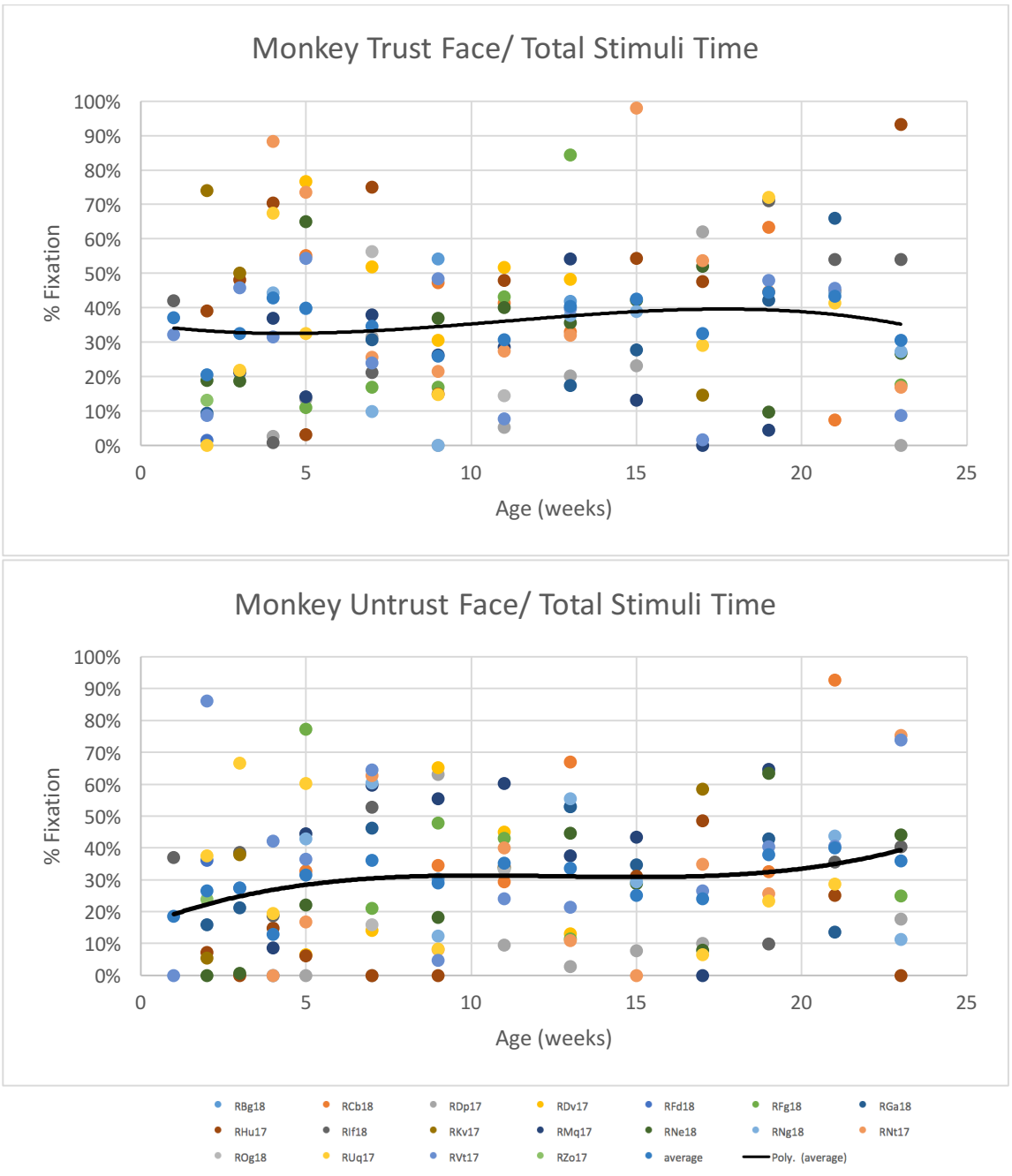

Figure 24: Raw data for percent time looking at monkey faces in relation to total stimuli time. Colored filled circles represent individual subject data and the black line represents the 3rd order polynomial line that best fit the average data points.

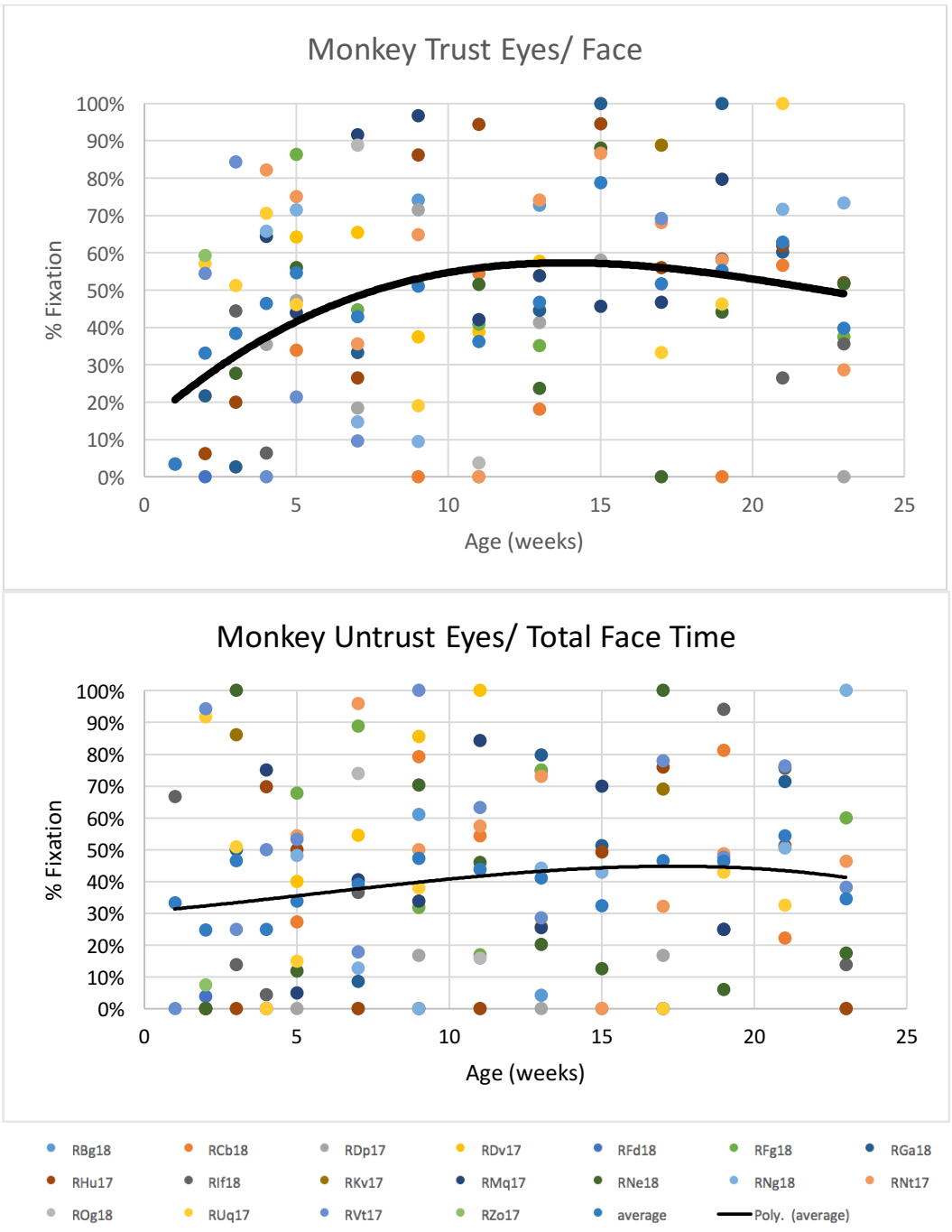

Figure 25: Percent time looking at monkey eyes in relation to total time looking at the whole face. Raw data for percent looking time at monkey eyes over time looking at the whole face for all subjects. Colored points represent individual subject data and the black line represents the 3rd order polynomial line of best fit for the average data points.

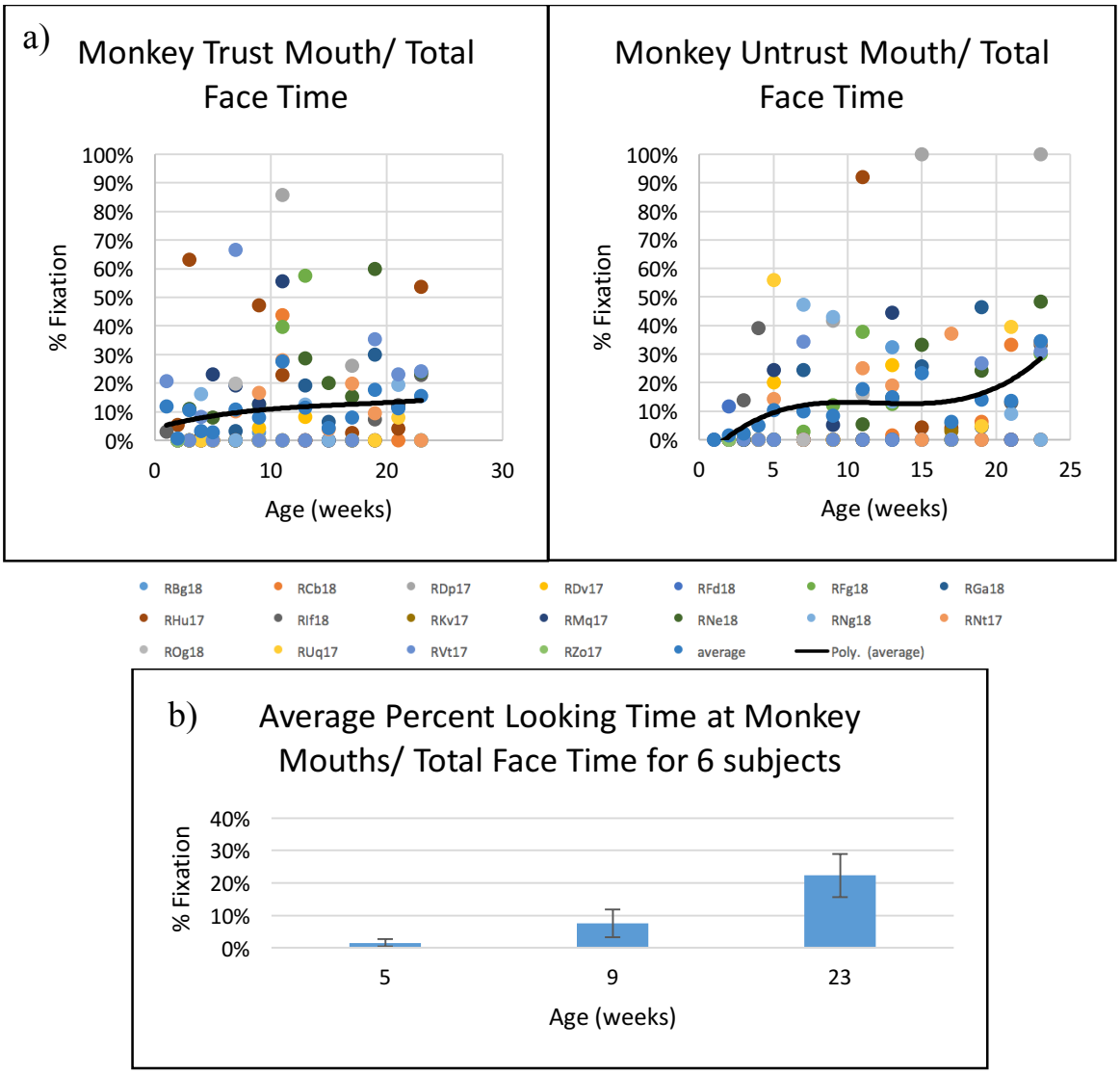

Figure 26: Percent time looking at monkey mouths in relation to total time looking at the whole face. a) Raw data for percent looking time at monkey eyes over time looking at the whole face for all subjects. Colored points represent individual subject data and the black line represents the 3rd order polynomial line of best fit for the average data points. b) Analysis of 6 subjects at 3 ages revealed a main effect of age ($F(2, 10)=5.245$, $p =0.028$, $\eta 2=0.512$), with the amount of time spent looking at the mouth of both the trustworthy and untrustworthy face increasing with age. The image shows the estimated marginal means for the percentage looking time at mouths in relation to total time looking at faces and the error bars represent the corrected SEM.

References

Adolph KE, Berger SE, Leo AJ (2011) Developmental continuity? Crawling, cruising, and walking. Dev Sci 14: 306-318.

Adolphs R, Tranel D, Damasio AR (1998) The human amygdala in social judgment. Nature 393: 470-474.

Augustine JR (1996) Circuitry and functional aspects of the insular lobe in primates including humans. Brain Research Reviews 22: 229-244.

Bachevalier J, Sanchez MM, Raper J, Stephens S, Wallen K (2016) The effects of neonatal amygdala lesions in rhesus monkeys living in a species-typical social environment. In: Living without an amygdala (eds: Amaral DG, Adolphs R), pp 186-217. New York, NY.

Barbas H, Zikopoulos B (2007) The prefrontal cortex and flexible behavior. Neuroscientist 13: 532-545.

Baron SG, Gobbini MI, Engell AD, Todorov A (2011) Amygdala and dorsomedial prefrontal cortex responses to appearance-based and behavior-based person impressions. Soc Cogn Affect Neurosci 6: 572-581.

Baron-Cohen S, Ring HA, Bullmore ET, Wheelwright S, Ashwin C, Williams SCR (2000) The amygdala theory of autism. Neuroscience and Biobehavioral Reviews 24: 355-364.

Bartels A, Zeki S (2000) The neural basis of romantic love. Neuroreport 11: 3829-3834.

Bauman MD, Iosif AM, Ashwood P, Braunschweig D, Lee A, Schumann CM, Van de Water J, Amaral DG (2013) Maternal antibodies from mothers of children with autism alter brain growth and social behavior development in the rhesus monkey. Translational Psychiatry 3:

Bjorklund DF (1987) A Note on Neonatal Imitation. Developmental Review 7: 86-92.

Boly M, Seth AK, Wilke M, Ingmundson P, Baars B, Laureys S, Edelman DB, Tsuchiya N (2013) Consciousness in humans and non-human animals: recent advances and future directions. Frontiers in Psychology 4:

Bonnefon JF, Hopfensitz A, De Neys W (2017) Can We Detect Cooperators by Looking at Their Face? Current Directions in Psychological Science 26: 276-281.

Bourgeois JP, Rakic P (1993) Changes of Synaptic Density in the Primary Visual-Cortex of the Macaque Monkey from Fetal to Adult Stage. Journal of Neuroscience 13: 2801-2820.

Bourgeois JP, Goldmanrakic PS, Rakic P (1994) Synaptogenesis in the Prefrontal Cortex of Rhesus-Monkeys. Cerebral Cortex 4: 78-96.

Brosnan SF, De Waal FB (2003) Monkeys reject unequal pay. Nature 425: 297-299.

Brothers L (1990) The Neural Basis of Primate Social Communication. Motivation and Emotion 14: 81-91.

Castellanos FX, Giedd JN, Berquin PC, Walter JM, Sharp W, Tran T, Vaituzis AC, Blumenthal JD, Nelson J, Bastain TM, Zijdenbos A, Evans AC, Rapoport JL (2001) Quantitative brain magnetic resonance imaging in girls with attention-deficit/hyperactivity disorder. Archives of General Psychiatry 58: 289-295.

Castellanos FX, Giedd JN, Marsh WL, Hamburger SD, Vaituzis AC, Dickstein DP, Sarfatti SE, Vauss YC, Snell JW, Lange N, Kaysen D, Krain AL, Ritchie GF, Rajapakse JC, Rapoport JL (1996) Quantitative brain magnetic resonance imaging in attention-deficit hyperactivity disorder. Archives of General Psychiatry 53: 607-616.

Chevalier N, Kurth S, Doucette MR, Wiseheart M, Deoni SCL, Dean DC, O'Muircheartaigh J, Blackwell KA, Munakata Y, LeBourgeois MK (2015) Myelination Is Associated with Processing Speed in Early Childhood: Preliminary Insights. Plos One 10:

Cogsdill EJ, Todorov AT, Spelke ES, Banaji MR (2014) Inferring character from faces: a developmental study. Psychol Sci 25: 1132-1139.

Coleman K, Pierre PJ (2014) Assessing Anxiety in Nonhuman Primates. Ilar Journal 55: 333-346.

Courchesne E, Carper R, Akshoomoff N (2003) Evidence of brain overgrowth in the first year of life in autism. JAMA 290: 337-344.

Craig AD (2009) How do you feel - now? The anterior insula and human awareness. Nature Reviews Neuroscience 10: 59-70.

Dahl CD, Wallraven C, Bulthoff HH, Logothetis NK (2009) Humans and Macaques Employ Similar Face-Processing Strategies. Current Biology 19: 509-513.

Dakin S, Frith U (2005) Vagaries of visual perception in autism. Neuron 48: 497-507.

de Waal FBM (2014) Natural normativity: The 'is' and 'ought' of animal behavior. Behaviour 151: 185-204.

Deaner RO, Khera AV, Platt ML (2005) Monkeys pay per view: Adaptive valuation of social images by rhesus macaques. Current Biology 15: 543-548.

Dettmer AM, Kaburu SSK, Byers KL, Murphy AM, Soneson E, Wooddell LJ, Suomi SJ (2016a) First-Time Rhesus Monkey Mothers, and Mothers of Sons, Preferentially Engage in Face-to-Face Interactions With Their Infants. American Journal of Primatology 78: 238-246.

Dettmer AM, Kaburu SSK, Simpson EA, Paukner A, Sclafani V, Byers KL, Murphy AM, Miller M, Marquez N, Miller GM, Suomi SJ, Ferrari PF (2016b) Neonatal face-to-face interactions promote later social behaviour in infant rhesus monkeys. Nature Communications 7:

Dobson SD (2012) Coevolution of Facial Expression and Social Tolerance in Macaques. American Journal of Primatology 74: 229-235.

Dzhelyova MP, Ellison A, Atkinson AP (2011) Event-related Repetitive TMS Reveals Distinct, Critical Roles for Right OFA and Bilateral Posterior STS in Judging the Sex and Trustworthiness of Faces. Journal of Cognitive Neuroscience 23: 2782-2796.

Emery NJ (2000) The eyes have it: the neuroethology, function and evolution of social gaze. Neuroscience and Biobehavioral Reviews 24: 581-604.

Engell AD, Todorov A, Haxby JV (2010) Common neural mechanisms for the evaluation of facial trustworthiness and emotional expressions as revealed by behavioral adaptation. Perception 39: 931-941.

Evrard HC, Forro T, Logothetis NK (2012) Von Economo Neurons in the Anterior Insula of the Macaque Monkey. Neuron 74: 482-489.

Ewbank MP, Jennings C, Calder AJ (2009) Why are you angry with me? Facial expressions of threat influence perception of gaze direction. Journal of Vision 9:

Ewing L, Caulfield F, Read A, Rhodes G (2015a) Perceived trustworthiness of faces drives trust behaviour in children. Developmental Science 18: 327-334.

Ewing L, Caulfield F, Read A, Rhodes G (2015b) Appearance-based trust behaviour is reduced in children with autism spectrum disorder. Autism 19: 1002-1009.

Farroni T, Csibra G, Simion G, Johnson MH (2002) Eye contact detection in humans from birth. Proceedings of the National Academy of Sciences of the United States of America 99: 9602-9605.

Ferrari PF, Paukner A, Ionica C, Suomi SJ (2009) Reciprocal Face-to-Face Communication between Rhesus Macaque Mothers and Their Newborn Infants. Current Biology 19: 1768-1772.

Frank MC, Vul E, Johnson SP (2009) Development of infants' attention to faces during the first year. Cognition 110: 160-170.

Frith C (2009) Role of facial expressions in social interactions. Philosophical Transactions of the Royal Society B: Biological Sciences 364: 3453-3458.

Frith CD, Frith U (1999) Cognitive psychology - Interacting minds - A biological basis. Science 286: 1692-1695.

Gabard-Durnam LJ, Flannery J, Goff B, Gee DG, Humphreys KL, Telzer E, Hare T, Tottenham N (2014) The development of human amygdala functional connectivity at rest from 4 to 23 years: a cross-sectional study. Neuroimage 95: 193-207.

Gauthier I, Klaiman C, Schultz RT (2009) Face composite effects reveal abnormal face processing in Autism spectrum disorders. Vision Research 49: 470-478.

Giedd JN, Rapoport JL (2010) Structural MRI of Pediatric Brain Development: What Have We Learned and Where Are We Going? Neuron 67: 728-734.

Giedd JN, Lalonde FM, Celano MJ, White SL, Wallace GL, Lee NR, Lenroot RK (2009) Anatomical Brain Magnetic Resonance Imaging of Typically Developing Children and Adolescents. Journal of the American Academy of Child and Adolescent Psychiatry 48: 465-470.

Gilmore JH, Shi F, Woolson SL, Knickmeyer RC, Short SJ, Lin WL, Zhu HT, Hamer RM, Styner M, Shen DG (2012) Longitudinal Development of Cortical and Subcortical Gray Matter from Birth to 2 Years. Cerebral Cortex 22: 2478-2485.

Gogtay N, Giedd JN, Lusk L, Hayashi KM, Greenstein D, Vaituzis AC, Nugent TF, Herman DH, Clasen LS, Toga AW, Rapoport JL, Thompson PM (2004) Dynamic mapping of human cortical development during childhood through early adulthood. Proceedings of the National Academy of Sciences of the United States of America 101: 8174-8179.

Graham AM, Buss C, Rasmussen JM, Rudolph MD, Demeter DV, Gilmore JH, Styner M, Entringer S, Wadhwa PD, Fair DA (2016) Implications of newborn amygdala connectivity for

fear and cognitive development at 6-months-of-age. Developmental Cognitive Neuroscience 18: 12-25.

Grossman M, Anderson C, Khan A, Avants B, Elman L, McCluskey L (2008) Neural basis for impaired action knowledge in amyotrophic lateral sclerosis. Neurology 70: A248-A248.

Grossmann T, Lloyd-Fox S, Johnson MH (2013) Brain responses reveal young infants' sensitivity to when a social partner follows their gaze. Developmental Cognitive Neuroscience 6: 155-161.

Grossmann T, Johnson MH, Lloyd-Fox S, Blasi A, Deligianni F, Elwell C, Csibra G (2008) Early cortical specialization for face-to-face communication in human infants. Proceedings of the Royal Society B-Biological Sciences 275: 2803-2811.

Guo K, Tunnicliffe D, Roebuck H (2010) Human spontaneous gaze patterns in viewing of faces of different species. Perception 39: 533-542.

Guo K, Robertson RG, Mahmoodi S, Tadmor Y, Young MP (2003) How do monkeys view faces? - a study of eye movements. Experimental Brain Research 150: 363-374.

Guo K, Meints K, Hall C, Hall S, Mills D (2009) Left gaze bias in humans, rhesus monkeys and domestic dogs. Animal Cognition 12: 409-418.

Harry B, Williams MA, Davis C, Kim J (2013) Emotional expressions evoke a differential response in the fusiform face area. Front Hum Neurosci 7: 692.

Hazlett HC, Gu H, Munsell BC, Kim SH, Styner M, Wolff JJ, Elison JT, Swanson MR, Zhu H, Botteron KN, Collins DL, Constantino JN, Dager SR, Estes AM, Evans AC, Fonov VS, Gerig G, Kostopoulos P, McKinstry RC, Pandey J, Paterson S, Pruett JR, Schultz RT, Shaw DW, Zwaigenbaum L, Piven J, The IN (2017) Early brain development in infants at high risk for autism spectrum disorder. Nature 542: 348.

Heimann M (1989) Neonatal Imitation, Gaze Aversion, and Mother Infant Interaction. Infant Behavior & Development 12: 495-505.

Herschkowitz N (2000) Neurological bases of behavioral development in infancy. Brain & Development 22: 411-416.

Hill J, Inder T, Neil J, Dierker D, Harwell J, Van Essen D (2010) Similar patterns of cortical expansion during human development and evolution. Proceedings of the National Academy of Sciences of the United States of America 107: 13135-13140.

Howell BR, Grand AP, McCormack KM, Shi YD, LaPrarie JL, Maestripieri D, Styner MA, Sanchez MM (2014) Early Adverse Experience Increases Emotional Reactivity in Juvenile Rhesus Macaques: Relation to Amygdala Volume. Developmental Psychobiology 56: 1735-1746.

Jezzini A, Rozzi S, Borra E, Gallese V, Caruana F, Gerbella M (2015) A shared neural network for emotional expression and perception: an anatomical study in the macaque monkey. Front Behav Neurosci 9: 243.

Johnson DK, Morris J, Galvin J (2008) Longitudinal analyses of cognition in dementia of the Alzheimer type, Parkinson's patients with and without dementia, and healthy controls. Neurology 70: A282-A282.

Johnson MH, Dziurawiec S, Ellis H, Morton J (1991) Newborns Preferential Tracking of Face-Like Stimuli and Its Subsequent Decline. Cognition 40: 1-19.

Jones BC, Hahn AC, Fisher CI, Wincenciak J, Kandrik M, Roberts SC, Little AC, DeBruine LM (2015) Facial coloration tracks changes in women's estradiol. Psychoneuroendocrinology 56: 29-34.

Joseph RM, Tanaka J (2003) Holistic and part-based face recognition in children with autism. J Child Psychol Psychiatry 44: 529-542.

Kaburu SSK, Paukner A, Simpson EA, Suomi SJ, Ferrari PF (2016) Neonatal imitation predicts infant rhesus macaque (Macaca mulatta) social and anxiety-related behaviours at one year. Scientific Reports 6:

Kanwisher N, Yovel G (2006) The fusiform face area: a cortical region specialized for the perception of faces. Philosophical Transactions of the Royal Society B-Biological Sciences 361: 2109-2128.

Klin A, Jones W (2008) Altered face scanning and impaired recognition of biological motion in a 15-month-old infant with autism. Developmental Science 11: 40-46.

Knickmeyer RC, Styner M, Short SJ, Lubach GR, Kang C, Hamer R, Coe CL, Gilmore JH (2010) Maturational Trajectories of Cortical Brain Development through the Pubertal Transition: Unique Species and Sex Differences in the Monkey Revealed through Structural Magnetic Resonance Imaging. Cerebral Cortex 20: 1053-1063.

Knickmeyer RC, Gouttard S, Kang CY, Evans D, Wilber K, Smith JK, Hamer RM, Lin W, Gerig G, Gilmore JH (2008) A Structural MRI Study of Human Brain Development from Birth to 2 Years. Journal of Neuroscience 28: 12176-12182.

Kolb B, Mychasiuk R, Muhammad A, Li YL, Frost DO, Gibb R (2012) Experience and the developing prefrontal cortex. Proceedings of the National Academy of Sciences of the United States of America 109: 17186-17193.

Kovacs-Balint Z, Feczko E, Pincus M, Howell B, Earl E, Li L, Steele J, Styner M, Bachevalier J, Fair D, Sanchez MM (2018) Early developmental trajectories of functional connectivity along the visual pathways in rhesus monkeys. Cerebral Cortex

Leon MI, Shadlen MN (1999) Effect of expected reward magnitude on the response of neurons in the dorsolateral prefrontal cortex of the macaque. Neuron 24: 415-425.

Lewkowicz DJ, Hansen-Tift AM (2012) Infants deploy selective attention to the mouth of a talking face when learning speech. Proceedings of the National Academy of Sciences of the United States of America 109: 1431-1436.

Li Q, Heyman GD, Mei J, Lee K (2017) Judging a Book by Its Cover: Children's Facial Trustworthiness as Judged by Strangers Predicts Their Real-World Trustworthiness and Peer Relationships. Child Dev

Liu C, Tian X, Liu H, Mo Y, Bai F, Zhao X, Ma Y, Wang J (2015) Rhesus monkey brain development during late infancy and the effect of phencyclidine: a longitudinal MRI and DTI study. Neuroimage 107: 65-75.

Ma FL, Xu F, Luo XM (2016) Children's Facial Trustworthiness Judgments: Agreement and Relationship with Facial Attractiveness. Frontiers in Psychology 7:

Machado CJ, Bachevalier J (2003) Non-human primate models of childhood psychopathology: the promise and the limitations. Journal of Child Psychology and Psychiatry 44: 64-87.

Maestripieri D, Wallen K (1997) Affiliative and submissive communication in rhesus macaques. Primates 38: 127-138.

Malkova L, Heuer E, Saunders RC (2006) Longitudinal magnetic resonance imaging study of rhesus monkey brain development. European Journal of Neuroscience 24: 3204-3212.

Markodimitraki M, Kypriotaki M, Ampartzaki M, Manolitsis G (2012) Effects of context and facial expression on imitation tasks in preschool children with autism. Early Child Development and Care 183:

Matsuzawa J, Matsui M, Konishi T, Noguchi K, Gur RC, Bilker W, Miyawaki T (2001) Age-related volumetric changes of brain gray and white matter in healthy infants and children. Cerebral Cortex 11: 335-342.

McFarland R, Roebuck H, Yan Y, Majolo B, Li W, Guo K (2013) Social Interactions through the Eyes of Macaques and Humans. Plos One 8:

Meltzoff AN, Moore MK (1977) Imitation of Facial and Manual Gestures by Human Neonates. Science 198: 75-78.

Meltzoff AN, Moore MK (1992) Early Imitation - within a Functional Framework - the Importance of Person Identity, Movement, and Development. Infant Behavior & Development 15: 479-505.

Mizuhiki T, Richmond BJ, Shidara M (2012) Encoding of reward expectation by monkey anterior insular neurons. J Neurophysiol 107: 2996-3007.

Molenberghs P, Brander C, Mattingley JB, Cunnington R (2010) The Role of the Superior Temporal Sulcus and the Mirror Neuron System in Imitation. Human Brain Mapping 31: 1316-1326.

Muschinski J, Feczko E, Brooks JM, Collantes M, Heitz TR, Parr LA (2016) The development of visual preferences for direct versus averted gaze faces in infant macaques (Macaca mulatta). Developmental Psychobiology 58: 926-936.

Nagai M, Kishi K, Kato S (2007) Insular cortex and neuropsychiatric disorders: A review of recent literature. European Psychiatry 22: 387-394.

Nahm FKD, Perret A, Amaral DG, Albright TD (1997) How do monkeys look at faces? Journal of Cognitive Neuroscience 9: 611-623.

Noonan T, Pinzur M, Paxinos O, Havey R, Patwardhin A (2005) Tibiotalocalcaneal arthrodesis with a retrograde intramedullary nail: A biomechanical analysis of the effect of nail length. Foot & Ankle International 26: 304-308.

Oberwelland E, Schilbach L, Barisic I, Krall SC, Vogeley K, Fink GR, Herpertz-Dahlmann B, Konrad K, Schulte-Ruther M (2017) Young adolescents with autism show abnormal joint attention network: A gaze contingent fMRI study. Neuroimage-Clinical 14: 112-121.

Parr LA, Heintz M (2009) Facial expression recognition in rhesus monkeys, Macaca mulatta. Animal Behaviour 77: 1507-1513.

Parr LA, Waller BM, Fugate J (2006) Emotional communication in primates: implications for neurobiology (vol 15, pg 716, 2005). Current Opinion in Neurobiology 16: 126-126.

Pascalis O, de Haan M, Nelson CA (2002) Is face processing species-specific during the first year of life? Science 296: 1321-1323.

Paxinos R, Mitchell JG (2000) A rapid Utermohl method for estimating algal numbers. Journal of Plankton Research 22: 2255-2262.

Payne C, Machado CJ, Bliwise NG, Bachevalier J (2010) Maturation of the Hippocampal Formation and Amygdala in Macaca mulatta: A Volumetric Magnetic Resonance Imaging Study. Hippocampus 20: 922-935.

Pinkham AE, Hopfinger JB, Pelphrey KA, Piven J, Penn DL (2008) Neural bases for impaired social cognition in schizophrenia and autism spectrum disorders. Schizophrenia Research 99: 164-175.

Prevost M, Brodeur M, Onishi KH, Lepage M, Gold I (2015) Judging strangers' trustworthiness is associated with theory of mind skills. Frontiers in Psychiatry 6:

Rae CL, Hughes LE, Anderson MC, Rowe JB (2015) The Prefrontal Cortex Achieves Inhibitory Control by Facilitating Subcortical Motor Pathway Connectivity. Journal of Neuroscience 35: 786-794.

Redcay E, Dodell-Feder D, Mavros PL, Kleiner M, Pearrow MJ, Triantafyllou C, Gabrieli JD, Saxe R (2013) Atypical brain activation patterns during a face-to-face joint attention game in adults with autism spectrum disorder. Human Brain Mapping 34: 2511-2523.

Reitsema LJ, Partrick KA, Muir AB (2016) Inter-Individual Variation in Weaning Among Rhesus Macaques (Macaca mulatta): Serum Stable Isotope Indicators of Suckling Duration and Lactation. American Journal of Primatology 78:

Rilling JK, Winslow JT, Kilts CD (2004) The neural correlates of mate competition in dominant male rhesus Macaques. Biol Psychiatry 56: 364-375.

Roth TL, Sullivan RM (2005) Memory of early maltreatment: neonatal behavioral and neural correlates of maternal maltreatment within the context of classical conditioning. Biol Psychiatry 57: 823-831.

Rowe JB, Eckstein D, Braver T, Owen AM (2008) How Does Reward Expectation Influence Cognition in the Human Brain? Journal of Cognitive Neuroscience 20: 1980-1992.

Rump KM, Giovannelli JL, Minshew NJ, Strauss MS (2009) The Development of Emotion Recognition in Individuals With Autism. Child Development 80: 1434-1447.

Sakagami M, Tsutsui K, Lauwereyns J, Koizumi M, Kobayashi S, Hikosaka O (2001) A code for behavioral inhibition on the basis of color, but not motion, in ventrolateral prefrontal cortex of macaque monkey. Journal of Neuroscience 21: 4801-4808.

Saleem KS 2012 A combined MRI and histology atlas of the rhesus monkey brain in stereotaxic coordinates. Journal

Saleem KS, Tanaka K (1996) Divergent projections from the anterior inferotemporal area TE to the perirhinal and entorhinal cortices in the macaque monkey. Journal of Neuroscience 16: 4757-4775.

Sallet J, Mars RB, Noonan MP, Andersson JL, O'Reilly JX, Jbabdi S, Croxson PL, Jenkinson M, Miller KL, Rushworth MFS (2011) Social Network Size Affects Neural Circuits in Macaques. Science 334: 697-700.

Sanchez MM (2006) The impact of early adverse care on HPA axis development: nonhuman primate models. Hormones and Behavior 50: 623-631.

Santos LR, Nissen AG, Ferrugia JA (2006) Rhesus monkeys, Macaca mulatta, know what others can and cannot hear. Animal Behaviour 71: 1175-1181.

Santos S, Almeida I, Oliveiros B, Castelo-Branco M (2016) The Role of the Amygdala in Facial Trustworthiness Processing: A Systematic Review and Meta-Analyses of fMRI Studies. Plos One 11:

Schobert AK, Corradi-Dell'Acqua C, Fruhholz S, van der Zwaag W, Vuilleumier P (2018) Functional organization of face processing in the human superior temporal sulcus: a 7T high-resolution fMRI study. Soc Cogn Affect Neurosci 13: 102-113.

Schultz RT, Gauthier I, Klin A, Fulbright RK, Anderson AW, Volkmar F, Skudlarski P, Lacadic C, Cohen DJ, Gore JC (2000) Abnormal ventral temporal cortical activity during face discrimination among individuals with autism and Asperger syndrome. Archives of General Psychiatry 57: 331-340.

Schwiedrzik CM, Zarco W, Everling S, Freiwald WA (2015) Face Patch Resting State Networks Link Face Processing to Social Cognition. Plos Biology 13:

Scott JA, Grayson D, Fletcher E, Lee A, Bauman MD, Schumann CM, Buonocore MH, Amaral DG (2016) Longitudinal analysis of the developing rhesus monkey brain using magnetic resonance imaging: birth to adulthood. Brain Structure & Function 221: 2847-2871.

Seltzer B, Pandya DN (1978) Afferent Cortical Connections and Architectonics of Superior Temporal Sulcus and Surrounding Cortex in Rhesus-Monkey. Brain Research 149: 1-24.

Shaw P, Kabani NJ, Lerch JP, Eckstrand K, Lenroot R, Gogtay N, Greenstein D, Clasen L, Evans A, Rapoport JL, Giedd JN, Wise SP (2008) Neurodevelopmental trajectories of the human cerebral cortex. Journal of Neuroscience 28: 3586-3594.

Shi YD, Budin F, Yapuncich E, Rumple A, Young JT, Payne C, Zhang XD, Hu XP, Godfrey J, Howell B, Sanchez MM, Styner MA (2017) UNC-Emory Infant Atlases for Macaque Brain Image Analysis: Postnatal Brain Development through 12 Months. Frontiers in Neuroscience 10:

Short SJ, Lubach GR, Karasin AI, Olsen CW, Styner M, Knickmeyer RC, Gilmore JH, Coe CL (2010) Maternal influenza infection during pregnancy impacts postnatal brain development in the rhesus monkey. Biol Psychiatry 67: 965-973.

Stephani C, Vaca GFB, Maciunas R, Koubeissi M, Luders HO (2011) Functional neuroanatomy of the insular lobe. Brain Structure & Function 216: 137-149.

Sterck EHM, Goossens BMA (2008) The meaning of "macaque" facial expressions. Proceedings of the National Academy of Sciences of the United States of America 105: E71-E71.

Styner M, Knickmeyer R, Joshi S, Coe C, Short SJ, Gilmore J (2007) Automatic brain segmentation in rhesus monkeys. 6512: 65122L-65122L-65128.

Sullivan RM (2017) Attachment Figure's Regulation of Infant Brain and Behavior. Psychodyn Psychiatry 45: 475-498.

Sullivan RM, Toubas P (1998) Clinical usefulness of maternal odor in newborns: soothing and feeding preparatory responses. Biol Neonate 74: 402-408.

Suomi SJ (2005a) Aggression and social behaviour in rhesus monkeys. Novartis Found Symp 268: 216-222; discussion 222-216, 242-253.

Suomi SJ (2005b) Mother-infant attachment, peer relationships, and the development of social networks in rhesus monkeys. Human Development 48: 67-79.

Suzuki WA, Amaral DG (1994) Perirhinal and parahippocampal cortices of the macaque monkey: cortical afferents. Journal of Comparative Neurology 350: 497-533.

Tarullo AR, Gunnar MR (2006) Child maltreatment and the developing HPA axis. Hormones and Behavior 50: 632-639.

Thompson-Schill SL, Ramscar M, Chrysikou EG (2009) Cognition Without Control: When a Little Frontal Lobe Goes a Long Way. Current Directions in Psychological Science 18: 259-263.

Todorov A, Baron SG, Oosterhof NN (2008) Evaluating face trustworthiness: a model based approach. Soc Cogn Affect Neurosci 3: 119-127.

Tsao DY, Moeller S, Freiwald WA (2008) Comparing face patch systems in macaques and humans. Proc Natl Acad Sci U S A 105: 19514-19519.

Uematsu A, Matsui M, Tanaka C, Takahashi T, Noguchi K, Suzuki M, Nishijo H (2012) Developmental Trajectories of Amygdala and Hippocampus from Infancy to Early Adulthood in Healthy Individuals. Plos One 7:

Ungerleider LG, Courtney SM, Haxby JV (1998) A neural system for human visual working memory. Proceedings of the National Academy of Sciences of the United States of America 95: 883-890.

Utevsky AV, Platt ML (2014) Status and the Brain. Plos Biology 12:

Wang J, Vachet C, Rumple A, Gouttard S, Ouziel C, Perrot E, Du G, Huang X, Gerig G, Styner M (2014) Multi-atlas segmentation of subcortical brain structures via the AutoSeg software pipeline. Front Neuroinform 8: 7.

Wincenciak J, Fincher CL, Fisher CI, Hahn AC, Jones BC, DeBruine LM (2015) Mate choice, mate preference, and biological markets: the relationship between partner choice and health preference is modulated by women's own attractiveness. Evolution and Human Behavior 36: 274-278.

Wing L, Gould J (1979) Severe Impairments of Social-Interaction and Associated Abnormalities in Children - Epidemiology and Classification. Journal of Autism and Developmental Disorders 9: 11-29.

Winston JS, Strange BA, O'Doherty J, Dolan RJ (2002) Automatic and intentional brain responses during evaluation of trustworthiness of faces. Nature Neuroscience 5: 277-283.

Xu F, Wu DC, Toriyama R, Ma FL, Itakura S, Lee K (2012) Similarities and Differences in Chinese and Caucasian Adults' Use of Facial Cues for Trustworthiness Judgments. Plos One 7:

Yi L, Pan JH, Fan YB, Zou XB, Wang XM, Lee K (2013a) Children with autism spectrum disorder are more trusting than typically developing children. Journal of Experimental Child Psychology 116: 755-761.

Yi L, Fan YB, Quinn PC, Feng C, Huang D, Li J, Mao GQ, Lee K (2013b) Abnormality in face scanning by children with autism spectrum disorder is limited to the eye region: Evidence from multi-method analyses of eye tracking data. Journal of Vision 13:

Zecevic N (1998) Synaptogenesis in layer I of the human cerebral cortex in the first half of gestation. Cerebral Cortex 8: 245-252.